INVESTIGATION OF A MEDIUM WITH A LARGE, NEGATIVE PARAMETER OF NONLINEARITY AND ITS APPLICATION TO THE ENHANCEMENT OF A COMPACT, OMNIDIRECTIONAL, PARAMETRIC SOURCE

A Thesis
Presented to
the Academic Faculty

by

Alexis Dumortier

In partial Fulfillment
of the requirements for the Degree of
Master of Science
In the School of Mechanical Enigneering

The George W. Woodruff School of Mechanical Engineering
Georgia Institute of Technology

June 2004

INVESTIGATION OF A MEDIUM WITH A LARGE, NEGATIVE PARAMETER OF NONLINEARITY AND ITS APPLICATION TO THE ENHANCEMENT OF A COMPACT, OMNIDIRECTIONAL, PARAMETRIC SOURCE

Approved:

David Trivett, Chairman

Dr. Peter Rogers

Dr. Yves Berthelot

Date Approved: June 17th 2004

To my parents

ACKNOWLEDGEMENTS

I wish to express my deepest gratitude to my advisor David Trivett whose help, support and patience were priceless for the completion of this thesis. His insight concerning the project proved to be an invaluable resource and I will always be indebted to him. I would also like to thank Peter Rogers for his enthusiastic support, his interest for this project and his valuable comments.

I wish to thank Yves Berthelot for serving on my committee. I am also very grateful to François Guillot for providing me with suggestions and explanations every time I needed them and for his inestimable support during the project. My gratitude is extended to Etienne Dufour and John Doane for their kindness and their help constructing the source.

I would like to thank my friends for the moral support they always provided during my Master: Guillaume Rigole, Solène Bellanger and all those that are not named here but not forgotten either. I cannot thank enough my parents and my family for their constant encouragements and for all they have done to make this experience possible. I am very grateful to Michel Rousseau and Jean-Marc Breteau who gave me the opportunity to complete this double degree ENSIM-GEORGIA TECH.

Finally, I thank Marie-Laure for all she means to me and for her encouragements during this enriching experience.

TABLE OF CONTENTS

ACKNOLEDGEMENTS iv

TABLE OF CONTENTS v

LIST OF FIGURES viii

LIST OF TABLES x

SUMMARY xi

CHAPTER I - INTRODUCTION 1

I.1. Overview and motivation for the thesis 1
I.2. Hypothesis and objectives 3
I.3. Organization of the dissertation 3

CHAPTER II - THEORETICAL BACKGROUND 5

II.1. Basic notions of wave propagation 5
II.1.1. Fundamental acoustic equations 5
II.1.2. Linear acoustics 9
II.1.3. Nonlinear acoustics 12

II.2. Nonlinear propagation 16
II.2.1. Distortion effects 16
II.2.2. Transfer of energy 19

CHAPTER III - THEORETICAL PREDICTIONS 20

III.1. Definition of the parametric array 20

III.2.Description of the model 21
III.2.1. Theory of the model 22
III.2.2. Introduction of the dispersion effects 25
III.2.3. Validation of the dispersion modelling 27

III.3. Initialization of the model 30
III.3.1. Inputs related to the initial signal 30
III.3.2. Inputs related to the nonlinear medium 33

III.4. Model predictions 35
III.4.1. Simulation of the nonlinear propagation 35
III.4.2. Contribution of the layer resonance 37
III.4.3. Other model predictions 41

CHAPTER IV - EXPERIMENTAL IMPLEMENTATION 43

IV.1. Preparation of the nonlinear medium 43

IV.2. Preliminary measurements 47

IV.3. Construction of the source 52
IV.3.1. Description of the source 52
IV.3.2. Assembling of the transducer 53
IV.3.3. Design and construction of the mold 55
IV.3.4. Design of the boot 57
IV.3.5. Assembly of the source 59

CHAPTER V - MEASUREMENTS 62

V.1 Experimental setup 63
V.1.1. Positioning of the source 63
V.1.2. Driving voltage applied to the transducer 64
V.1.3. Data acquisition 65

V.2. Processing of the data 67
V.2.1. Filtering of the signal 69
V.2.2. Evaluation of the sound pressure level 70
V.2.3. Enhancement of the sound pressure level 70
V.2.4. Comparison with the model prediction 71

CHAPTER VI - CONCLUSION 73

VI.1. Summary of the work 73
VI.2. Results 75
VI.3. Future work 75

APPENDIX A - Simulation program 77

APPENDIX B - Transducer F56 81

APPENDIX C - Xanthan gel recipe 82

APPENDIX D - Hydrophones B&K8103 83

REFERENCES 84

LIST OF FIGURES

Figure II.1 - Distortion process in a medium with a negative coefficient of nonlinearity 17

Figure II.2 - Distortion process in a medium with a positive coefficient of nonlinearity 18

Figure II.3 - Harmonic behavior of an initially sinusoidal signal 19

Figure III.1 - Pulse profile achieved with 29
a) Nonlinear effects only
b) Dispersion effects only

Figure III.2 - Propagation of a soliton 29

Figure III.3 - Sound speed dependence on the pressure at 25° C 34

Figure III.4 - Amplitude of the particle velocity of the difference frequency and fundamentals 36

Figure III.5 - Evaluation of the gain factor 37

Figure III.6 - Gain factor as a function of the frequency 40

Figure IV.1 - Measurement of the static bulk modulus of the nonlinear medium. 48

Figure IV.2 - Change of volume in the vessel as a function of the pressure 49

Figure IV.3 - Description of the source 52

Figure IV.4 - Expansion undergone by a shell element 53

Figure IV.5 - Assembly and electrical connections of the transducer 54
a) Cross section
b) Front view

Figure IV.6 - Assembly of the transducer 55

Figure IV.7 - Casting of the plaster mold 56

Figure IV.8 - Plaster mold 56

Figure IV.9 - Casting of the rubber boot 57

Figure IV.10 - Hemispheric rubber boot 58

Figure IV.11 - Assembly of the source 59

Figure IV.12 - Source with medium in the bottom half of the boot 60

Figure IV.13 - Completed source 61

Figure V.1 - Source submerged in the water tank 62

Figure V.2 - Experimental setup 63

Figure V.3 - Driving voltage applied to the transducer 65

Figure V.4 - Signal radiated by the source at a depth of 6.5m (referred to 1m) 67

Figure V.5 - Difference frequency component at a depth of 6.5m 69

LIST OF TABLES

Table II.1: Values of the nonlinear parameter β and the sound speed c_0 for the medium castor oil-microspheres 34

SUMMARY

Nonlinear acoustic media for implementations of parametric generation of low frequencies has so far been restricted to small values of the parameter B/A, typically between 3 and 13.

Parametric amplification, defined as the generation of a low difference frequency signal resulting from the nonlinear interactions of two higher frequency fundamentals is enhanced by medium with a large coefficient of nonlinearity and low sound speed. The acoustic properties of a highly nonlinear medium were estimated and introduced in a numerical model, to evaluate the parametric amplification induced by a thin layer of such material in contact with a spherical transducer.

The numerical model predicted a significant enhancement of the sound pressure level for the difference frequency component relative to that obtained when the transducer is driven linearly at the difference frequency. A source was then constructed to compare the theoretical predictions with experimental values and an enhancement of 17dB compared to the linear operation of the transducer was measured. The difference between the parametric amplification achieved with the nonlinear medium and the parametric amplification that would be obtained in water is 73dB.

CHAPTER I

INTRODUCTION

I.1. Overview and motivation for the thesis

The research presented in this thesis belongs to the area of nonlinear acoustics. Nonlinear acoustics is characterized by the distortion of waves of large amplitude as they propagate through media. The experimental study of such distortion effects in fluids is restricted to high frequency by low values of the nonlinear parameter B/A in most media.

The development of media with large coefficients of nonlinearity would broaden the possibility of nonlinear applications, such as the parametric amplification, which is characterized by the generation of a low difference frequency signal from the nonlinear interactions of two high frequency signals.

The parametric generation of the difference frequency depends strongly upon the nonlinear properties of the medium. Much effort had been directed toward the development of stable media with high coefficient of nonlinearity. It has been well established [1][2], that the presence of bubbles in a fluid contributes to parametric amplification by increasing the value of B/A when the frequency is close to the resonant frequency of the bubbles [3]. Asata reported [4] on a medium that consists of

microcapsules mixed in a silicone rubber allowing a parametric amplification due to the resonant oscillations of the microcapsules. However, using such high frequencies to enhance the nonlinearity parameter is often impractical.

The present research expands on the work conducted by two past master students at the Georgia Institute of Technology, Hervé Pinçon [5] and Olivier Pauly [6]. In their research, they investigated a medium with a large and negative coefficient of nonlinearity. Hervé Pinçon characterized a mixture of Castor oil and microspheres by measuring the dependence of the sound speed on the pressure, which determines the first term of the parameter B/A. Olivier Pauly measured the dependence of the sound speed on the temperature and therefore deduced the second term of the parameter.

A medium, suitable for a practical implementation, with properties similar to those of the mixture of Castor Oil - microspheres will be investigated and used to achieve the parametric amplification of a low frequency signal and improve the performances of a low frequency projector.

I.2. Hypothesis and objectives

Our hypothesis was that a thin layer of a material with a large coefficient of nonlinearity could be used on the surface of a transducer to improve its performances at low frequency by inducing parametric amplification.

Based on this hypothesis, the present work had three main goals:

- Predict the performances of a source consisting of a transducer encapsulated in a thin layer of nonlinear medium.

- Develop a nonlinear medium suitable for the construction of the source.

- Construct the source, measure its performance, and compare it to the model predictions.

I.3. Organization of the dissertation

The present dissertation is divided as follows:

The second chapter introduces the fundamental principles of linear and nonlinear acoustics and expounds the transfer of energy resulting from the distortion processes

upon which the principle of the source is based in order to facilitate the comprehension of the numerical model described in the following chapter.

The third chapter is devoted to the detailed description of a model used to simulate the acoustic propagation of finite amplitude waves in a nonlinear medium and provides numerical predictions of the performances of the source. The underlying assumptions made prior in the use of the model and the results of the simulations are detailed.

In the fourth chapter, a nonlinear medium suitable for practical implementations is investigated. The measurements of its static properties are followed by a description of the construction of the source using this material.

The fifth chapter presents an experiment conducted to evaluate the sound pressure level radiated by the source and compares its performances with the theoretical predictions and with the performances of the transducer driven linearly.

The sixth chapter concludes the dissertation. It summarizes the work, emphasizes the main results and proposes further developments based on the present project.

CHAPTER II

THEORETICAL BACKGROUND

This chapter describes the basic concepts and principles of linear as well as non-linear acoustics in order to provide a better understanding of the experimental results discussed in the following sections.

II.1. Basic notions of wave propagation

II.1.1. Fundamental acoustic equations

The behavior of a fixed volume of fluid can be described by its pressure, p, density, ρ, fluid velocity, v, and entropy, s. The conservation of mass, Euler equation and equation of state are the fundamental acoustic equations that relate these variables and yield the derivation of both linear and nonlinear acoustic equations.

The conservation of mass states that the total mass leaving a volume V (of external surface S) per unit time must be equal to the rate of change of the mass in the volume. The mathematical formulation of this statement is given by the following equation:

$$\oint_S \rho \vec{v}.d\vec{s} = \frac{\partial}{\partial t}\int_V \rho dV \qquad \text{(II.1)}$$

where the left hand side represents the mass leaving the volume per unit time and the right hand side the rate of change of the mass in the volume. The surface integral of the left part of the equation can be converted to a volume integral using Green's theorem and the previous relation simplifies as:

$$\int_V \left[\frac{\partial \rho}{\partial t} + \nabla \cdot (\rho v)\right] dV = 0 \qquad \text{(II.2)}$$

Since this equation is valid for any volume, the conservation of mass is given by

$$\frac{\partial \rho}{\partial t} + \nabla \cdot (\rho v) = 0 \qquad \text{(II.3)}$$

The equation for the conservation of the momentum, also called Euler's equation of motion, can be derived from the equation of motion of a volume element in the fluid given by:

$$\rho \frac{\partial v}{\partial t} = -\nabla \cdot p \qquad \text{(II.4)}$$

where the left hand side represents the acceleration of a unit volume and the right hand side the external forces exerted on this unit volume. This equation assumes no thermo-viscous losses which can be justified by the fact that the fluid is considered ideal.

The change in the velocity can be expressed as a sum of two contributions:

$$\frac{dv}{dt} = \left(\frac{\partial v}{\partial t}\right) + (\vec{v} \cdot \nabla)\vec{v} \tag{II.5}$$

where the first term of the right hand side represents the change of velocity of that unit volume relative to a fixed reference frame and the second term the change due to any gradient in the velocity field. The conservation of momentum can also be written as

$$\rho \frac{Dv}{Dt} + \nabla p = 0 \tag{II.6}$$

The equation of states relates the pressure to the density of the fluid and its entropy:

$$p = p(\rho, s) \tag{II.7}$$

These three equations provide a general description of the behavior of fluids. However the derivation of the linear acoustic equations requires several specific assumptions detailed in the following section.

II.1.2. Linear acoustics

The propagation of an acoustic wave in a homogenous medium disturbs its ambient state defined by its pressure, density and fluid velocity (p_0, ρ_0, v_0). Therefore the resulting total density and pressure can be expressed as a sum of the disturbance and the ambient value as follows:

$$p = p_0 + p' \tag{II.8}$$

$$\rho = \rho_0 + \rho' \tag{II.9}$$

where p' and ρ' represent respectively the acoustic contribution to the total pressure and density introduced by the disturbance. For simplicity, the fluid is considered quiescent; which means that its ambient fluid velocity is constant and equal to zero. Therefore the fluid velocity is given by

$$v = v' \tag{II.10}$$

where v' represents the acoustic contribution.

Substituting these variables into the conservation of mass equation yields the following:

$$\frac{\partial(\rho_0 + \rho')}{\partial t} + \nabla \cdot [(\rho_0 + \rho')v'] = 0 \qquad \text{(II.11)}$$

The linear approximation states that the deviation from the ambient state variables are of very small amplitude. Therefore the second and higher order products of these quantities can be neglected and the preceding equation becomes:

$$\frac{\partial \rho'}{\partial t} + \rho_0 \nabla \cdot v' = 0 \qquad \text{(II.12)}$$

The same process applied to the conservation of momentum equation gives:

$$(\rho_0 + \rho')\left(\frac{\partial}{\partial t} + v' \cdot \nabla\right)v' = -\nabla(p_0 + p') \qquad \text{(II.13)}$$

Once the higher order terms are neglected, the equation simplifies to:

$$\rho_0 \frac{\partial v'}{\partial t} + \nabla p' = 0 \qquad \text{(II.14)}$$

The equation of state becomes:

$$p_0 + p' = p(\rho_0 + \rho', s_0) \tag{II.15}$$

and can be expand with a Taylor-series to give:

$$p' = \left(\frac{\partial p}{\partial \rho}\right)_{s_0,\rho_0} .\rho' + \frac{1}{2}\left(\frac{\partial^2 p}{\partial \rho^2}\right)_{s_0,\rho_0} .(\rho')^2 + \ldots \tag{II.16}$$

The expansion of the equation of state with partial derivatives evaluated at s_0 is justified by making the assumption that the entropy remains constant and equal for all the particles in the fluid. This last assumption is consistent with the fact that the fluid considered is homogenous.

Neglecting the higher order terms yields:

$$p' = c^2 \rho' \tag{II.17}$$

given that:

$$c^2 = \left(\frac{\partial p}{\partial \rho}\right)_{s_0,\rho_0} \tag{II.18}$$

where c represents the speed of sound in the medium. Combining these equations one obtains the linear wave equation:

$$\nabla^2 p - \frac{1}{c^2}\frac{\partial^2 p}{\partial t^2} = 0 \qquad \text{(II.19)}$$

II.1.3. Nonlinear acoustics

The disturbance caused in linear acoustic, by a traveling wave, was considered small enough to allow for the neglecting of several cross-product terms. However, for waves of larger amplitude, these terms need to be retained in the calculations and lead to the nonlinear acoustic equations.

The equation of state can then be reformulated as:

$$p' = A.\frac{\rho'}{\rho_0} + \frac{B}{2!}.\left(\frac{\rho'}{\rho_0}\right)^2 + \frac{C}{3!}.\left(\frac{\rho'}{\rho_0}\right)^3 + \ldots \qquad \text{(II.20)}$$

where A, B and C refer to the coefficients of the Taylor series expansion. These coefficients are given by:

$$A = \rho_0\left(\frac{\partial p'}{\partial \rho}\right)_{s_0,\rho_0} \qquad B = {\rho_0}^2\left(\frac{\partial^2 p'}{\partial \rho^2}\right)_{s_0,\rho_0} \qquad C = {\rho_0}^3\left(\frac{\partial^3 p'}{\partial \rho^3}\right)_{s_0,\rho_0}$$

The coefficient of nonlinearity is defined [7] to be equal to:

$$\beta = 1 + \frac{B}{2A} \tag{II.21}$$

According to the previous development, the propagation of a plane wave traveling in the positive x direction in a homogeneous and lossless medium is determined by the following equations\

$$\frac{\partial \rho}{\partial t} + \frac{\partial (\rho v)}{\partial x} = 0 \tag{II.22}$$

$$\rho\left(\frac{\partial v}{\partial t} + v\frac{\partial v}{\partial x}\right) = -\frac{\partial p}{\partial x} \tag{II.23}$$

$$p = p(\rho, s) \tag{II.24}$$

Assuming the particle velocity is a single valued function of the pressure one can write

$$\frac{\partial v}{\partial t} = \left(\frac{dv}{dp}\right).\frac{\partial p}{\partial t} \tag{II.25}$$

when substituted in the mass conservation equation and Euler equation, this gives

$$\frac{d\rho}{dp}\frac{\partial p}{\partial t}+\frac{d(\rho v)}{dp}\frac{\partial p}{\partial x}=0 \tag{II.26}$$

$$\rho\frac{dv}{dp}\frac{\partial p}{\partial t}+\left(\rho v\frac{dv}{dp}+1\right)\frac{\partial p}{\partial x}=0 \tag{II.27}$$

The solution of this system is possible only if the determinant of the coefficients is equal to zero. This requirement, associated with $\frac{d\rho}{dp}=\frac{1}{c^2}$, leads to $\frac{dv}{dp}=\frac{1}{\rho c}$ which, when introduced in equation (II.27) gives:

$$\frac{\partial p}{\partial t}+(v+c)\frac{\partial p}{\partial x}=0 \tag{II.28}$$

Since the ambient value of the pressure depends neither on time nor on position, p can be replaced in the previous equation by the acoustic contribution p' to yield a solution of the form:

$$p'=f(x+(c+v)t) \tag{II.29}$$

The total speed of each location of the wave profile results from the sum of the speed of sound and the particle velocity. The dependence of each of these quantities on the acoustic pressure is given by

$$v \approx \frac{p'}{\rho_0 c_0} \qquad c \approx c_0 + \left(\frac{\partial c}{\partial p}\right)_{s_0, p_0} p'$$

Therefore the total traveling speed of each pressure location of the wave profile can be expressed as

$$c + v \approx c_0 + \frac{\beta p'}{\rho_0 c_0} \tag{II.30}$$

where

$$\beta = 1 + \left(\rho_0 c_0 \frac{\partial c}{\partial p}\right)_{s_0, p_0} \tag{II.31}$$

II.2. Nonlinear propagation

A harmonic wave traveling in a nonlinear medium is subjected to distortion effects proportional to the coefficient of nonlinearity. This cumulative process modifies the wave profile and may eventually leads to a shock wave, depending upon linear attenuation levels.

II.2.1. Distortion effects

The propagation of a sine wave is analyzed to illustrate the distortion process in the case of a medium with a negative coefficient of nonlinearity and in a medium with a positive coefficient of nonlinearity.

As the wave propagates in a medium with a negative coefficient of nonlinearity, the speed of the positive pressure region of the wave profile decreases with increasing distance whereas the speed of the negative region increases relative to the speed of sound.

Since this change is proportional to the absolute value of the pressure, the distortion process does not affect the speed of the zero pressure locations of the profile that remains constant and equal to the speed of sound at the ambient hydrostatic pressure.

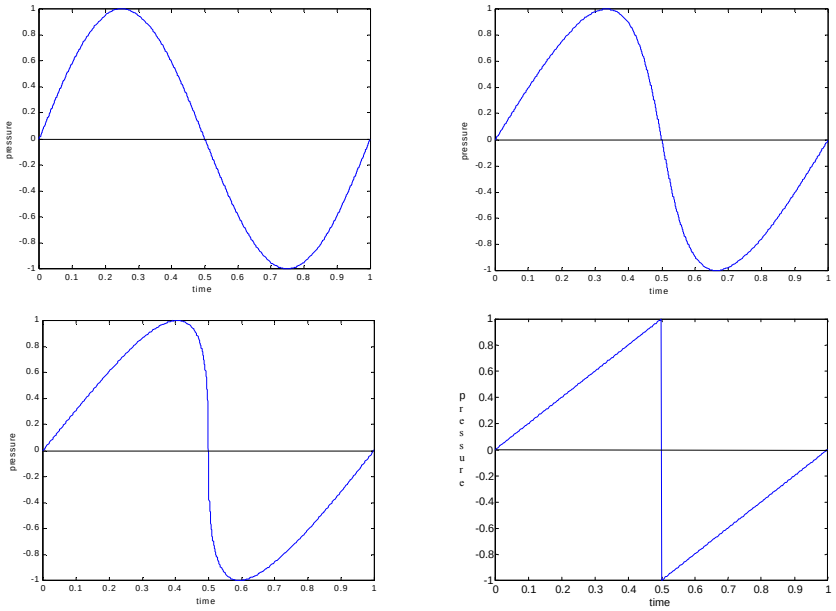

Figure II.1 - Distortion process in a medium with a negative coefficient of nonlinearity

As the wave reaches the shock distance, a discontinuity appears in the profile corresponding to an abrupt change of pressure from a positive to a negative value. This results in the propagation of a rarefaction shock wave.

In a medium with a positive coefficient of nonlinearity the speed of the positive pressure regions of the wave profile increases with increasing distance whereas the speed of the negative pressure regions decreases.

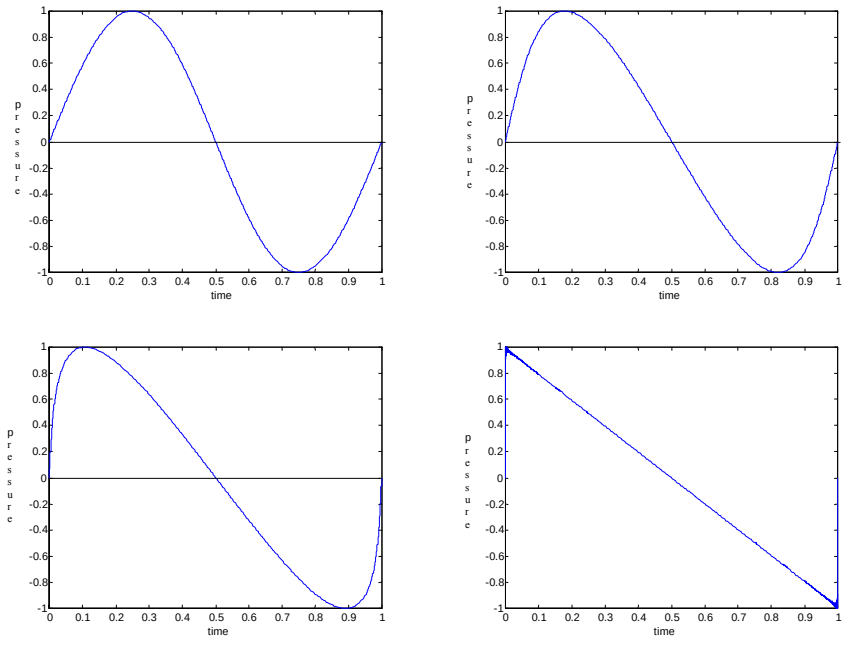

Figure II.2 - Distortion process in a medium with a positive coefficient of nonlinearity

When the shock distance is reached a wave front appears and the wave keeps propagating with an N-wave profile, subjected to the dissipation effects.

The discontinuity distance depends on the coefficient of nonlinearity of the medium as well as on the type of spreading corresponding to the geometry of the source.

II.2.2. Transfer of energy

A sound wave traveling in a nonlinear medium gives up energy either dissipated in the medium or transferred to create new frequency components. The parametric array, detailed in the following section, is based on the generation of new frequency components from those already existing and takes advantage of the distortion process that allows the energy of the signal to translate from its fundamental to the harmonics.

The transfer of energy is illustrated by evaluating the Fourier transform of a signal initially sinusoidal as it propagates in a nonlinear medium. As the amplitude of the fundamental decreases with increasing distances, the amplitude of the harmonics increases until the energy of the fundamental becomes too small to compensate for spreading losses or linear attenuation.

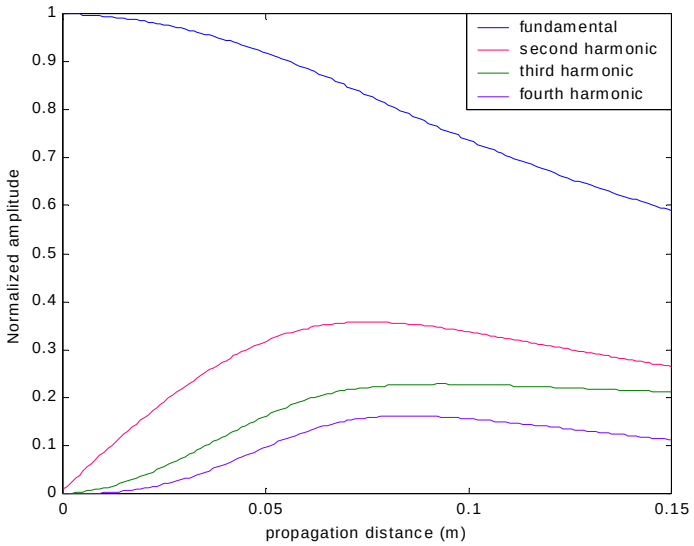

Figure II.3 - Harmonic behavior of an initially sinusoidal signal

CHAPTER III

THEORETICAL PREDICTIONS

As part of the design process for the omnidirectional, parametric array, a finite amplitude wave propagation model was used to calculate the level of difference frequency generated by propagating through the nonlinear medium. The first section defines the parametric array in order to provide a better understanding of the modeling detailed in the following sections of this chapter.

III.1. Definition of the parametric array

The parametric acoustic array was initially described by Westervelt [8] and consists of a piston transducer simultaneously generating two high frequency signals, referred to as the primaries frequencies, whose energy is confined to collimated superimposed beams, which interact nonlinearly to produce the sum and the difference frequency components, referred to as the secondary waves, as well as other nonlinearly generated harmonic waves.

The amplitude of the nonlinearly generated components increases until both the linear and nonlinear losses decrease the amplitude of the primaries to a low level and the propagation can be considered a linear process. The difference frequency is chosen small, relative to the primary frequencies, so that one obtains a highly collimated, low frequency source from a small diameter transducer. The linear losses are significantly less for low frequency acoustic propagation in the ocean, and a parametric array produces a compact directional source.

III.2. Description of the model

The distortion processes undergone by a wave traveling in a nonlinear medium can be viewed from two different perspectives and therefore modeled with different approaches. Khoklov [9] investigated the "slowly changing profile" method that treats the distortion effects in the time domain (requiring that attention be paid to preventing multi-valued profiles when the wave approaches the shock distance) while introducing absorption as well as geometrical spreading effects in the frequency domain. However, this type of method is computationally time-consuming due to the need to repeatedly change from the time domain to the frequency domain to perform the computations.

Trivett and Van Buren [10] eliminated this issue in an approach that determines the harmonic content of finite amplitude waves, through a stepwise process, exclusively in the frequency domain. A MATLAB® version of the program (see Appendix A) was

used in the present investigation and modified from the original FORTRAN program to take into account dispersion.

III.2.1. Theory of the model

The generalized Burger equation is first introduced as a valid nonlinear wave equation for a one dimensional, progressive wave [10]:

$$\frac{\partial U}{\partial r} + \left(\frac{a}{r}\right)U - \frac{\beta U}{{c_0}^2}\frac{\partial U}{\partial \tau} = 0 \qquad \text{(III.1)}$$

where U is the particle velocity, r the distance to the center of the source, β the nonlinear parameter, c_0 the sound speed in the medium and τ the retarded time. The value of the geometrical spreading factor, a, depends on the geometry of the one-dimensional wave considered:

$a = 0$	for planar waves
$a = 1/2$	for cylindrical waves
$a = 1$	for spherical waves

The present investigation is concerned with spherical waves requiring the setting of a to unity. It is obvious from equation III.1 that the nonlinear effects on the wave propagation represented by the product of U and $\partial U/\partial \tau$ are enhanced for media with a

large nonlinear parameter β and small speed of sound. Therefore these parameters will be of vital importance when choosing a suitable nonlinear medium for the source. Arbitrary linear attenuation, in the medium, is introduced by adding a term to the right hand side of equation III.1 transforming it into:

$$\frac{\partial U}{\partial r}+\left(\frac{1}{r}\right)U-\frac{\beta U}{{c_0}^2}\frac{\partial U}{\partial \tau}=-\alpha(\omega)U \qquad \text{(III.2)}$$

The calculations performed assumed that the frequency dependence of the attenuation coefficient varied quadratically, to prevent a numerical instability due to the high levels of nonlinearity, although as it will be seen, the linear attenuation is of little importance due to the large and dominating nonlinear attenuation and the short distances involved.

The equation is solved by introducing a trial solution in the form of a Fourier series:

$$U(r,\tau)=\sum_{k=1}^{\infty}\left(\frac{r_0}{r}\right)\{G_k\sin(k\omega_0\tau)+H_k\cos(k\omega_0\tau)\}\exp[-\alpha_k(r-r_0)] \qquad \text{(III.3)}$$

Where G_k and H_k refer to the amplitude components of the kth harmonic, α_k the corresponding linear absorption coefficient and ω_0 the fundamental frequency. Introducing the trial solution into equation (III.2) yields the following system of equations:

$$\frac{\partial G_k}{\partial r} = \frac{\beta\omega_0}{2{c_0}^2}\left(\frac{r_0}{r}\right)\left\{\sum_{m=1}^{k-l} m\left(G_{k-m}G_m - H_{k-m}H_m\right).\exp\left[-\left(\alpha_{k-m}+\alpha_m-\alpha_k\right)\left(r-r_0\right)\right]\right.$$

$$\left. - k\sum_{m=1}^{\infty}\left(G_{k+m}G_m + H_{k+m}H_m\right).\exp\left[-\left(\alpha_{k+m}+\alpha_m-\alpha_k\right)\left(r-r_0\right)\right]\right\} \qquad \text{(III.4)}$$

$$\frac{\partial H_k}{\partial r} = \frac{\beta\omega_0}{2{c_0}^2}\left(\frac{r_0}{r}\right)\left\{\sum_{m=1}^{k-l} m\left(H_{k-m}G_m - H_m G_{k-m}\right).\exp\left[-\left(\alpha_{k-m}+\alpha_m-\alpha_k\right)\left(r-r_0\right)\right]\right.$$

$$\left. + k\sum_{m=1}^{\infty}\left(H_m G_{k+m} - H_{k+m}G_m\right).\exp\left[-\left(\alpha_{k+m}+\alpha_m-\alpha_k\right)\left(r-r_0\right)\right]\right\} \qquad \text{(III.5)}$$

The numerical integration of equations (III.4) and (III.5) requires the truncation of the infinite series to a limited number of components for the calculations. As illustrated in the section II.2.2, the nonlinear propagation of a signal implies energy transfers from the lower to the higher harmonics. Therefore the number of terms retained needs to be large enough so that the amplitude of the last harmonic components retained remains small.

In addition, a number of the highest harmonics retained in the series must be stepwise reduced in level to prevent numerical instabilities caused by an accumulation of energy,

which then would propagates back to the lower harmonics. The two previous equations are stepwise, numerically integrated using the first order Runge Kutta method to provide the amplitude of each frequency component.

III.2.2. Introduction of the dispersion effects

In order to model more accurately the nonlinear propagation, the initial program was modified to take into account dispersion effects. The frequency dependence of the sound speed, typical of dispersive media, is best introduced through a stepwise process.

The dispersion is introduced into the model by first setting the frequency dependence of the sound speed, and then computing its value for each of the harmonics. The lowest frequency component considered in the program, which is also the slowest, is the difference frequency and its sound speed is set equal to c_0.

As each harmonic component propagates in the nonlinear medium, its phase changes relative to that of the difference frequency component. For the n^{th} harmonic, the phase shift introduced over a single step is computed as:

$$\Delta\phi_n = \frac{2\pi f_n * \Delta x}{c_0} - \frac{2\pi f_n * \Delta x}{c_0 + n\Delta c} \qquad \text{(III.6)}$$

where f_n is the frequency of the nth harmonic, c_0 the speed of sound of the difference frequency, Δc the speed shift per harmonic step, and Δx the stepsize. The same phase shift can also be expressed as:

$$\Delta\phi_n = \left(\frac{2\pi n f_d}{c_0} \left(1 - \left(\frac{c_0}{c_0 + n\Delta c} \right) \right) \right) * \Delta x \qquad \text{(III.7)}$$

where f_d is the difference frequency.

Once the coefficients G_k and H_k have been modified to account for the nonlinear and dissipative process, the dispersion is introduced in the solution (III.3) as follows:

$$U(r,\tau) = \sum_{k=1}^{\infty} \left(\frac{r_0}{r} \right) \{ G_k \sin(k\omega_0\tau - \Delta\phi_k) + H_k \cos(k\omega_0\tau - \Delta\phi_k) \} \exp[-\alpha_k (r - r_0)] \qquad \text{(III.8)}$$

Therefore the modified amplitudes of G_k and H_k noted G'_k and H'_k can be expressed as:

$$G'_k = G_k \cos(\Delta\phi_k) + H_k \sin(\Delta\phi_k) \qquad \text{(III.9)}$$

$$H'_k = H_k \cos(\Delta\phi_k) - G_k \sin(\Delta\phi_k) \qquad \text{(III.10)}$$

The program keeps track of the amplitude of the frequency components by saving them in text files. Once the signal has propagated over a distance of interest, the waveform can be rebuilt, if needed, in the time domain from the components of the Fourier series G_k and H_k.

III.2.3. Validation of the dispersion modeling

The model described in the section III.2 is assessed and validated by simulating the propagation of a soliton, a wave whose shape remains unchanged as it propagates in a medium where nonlinear and dispersion effects are balanced [11]. The shape of the pulse is a solution of the equation:

$$\frac{\partial U}{\partial t} + U\frac{\partial U}{\partial x} = \mu\frac{\partial^3 U}{\partial x^3} \qquad \text{(III.11)}$$

where U is the particle velocity, x is the distance to the source and μ is related to the wave number k and the frequency ω by:

$$\frac{\omega}{k} = c_0 - \mu k^2 \qquad \text{(III.12)}$$

Equation (III.11) expresses the balance between the distortions caused by the nonlinear propagation on the left hand side and the dispersion on the right hand side.

The solution of equation (III.11) is given by:

$$p(t) = -\frac{1}{\cosh^2(\omega t)} \tag{III.13}$$

The Fourier series of the pulse given by (III.13) is evaluated to determine the value of the coefficients, G_k and H_k, for use in the simulation program. The pulse is a transient signal however the computation of the Fourier series assumes a periodic signal. To minimize the impact, the transform is performed on a long window consisting of the pulse and a long series of zero's.

As the pulse propagates, the dispersion tends to retard the peak of the pulse whereas the nonlinear effects tend to advance it. The simulation was repeated a large number of time to adjust each type of distortion until the profile of the pulse remained roughly the same over a propagation distance equal to a large number of wavelengths. The soliton obtained with the simulation program does not have exactly the same profile as the initial pulse due the limited number of harmonics retained for the calculations. The amplitude of the peak is reduced by the linear losses and some oscillations that appear after the pulse result from the dispersion effects. However it clearly exhibits a balance between the two types of distortion shown on figure III.1 a) and b).

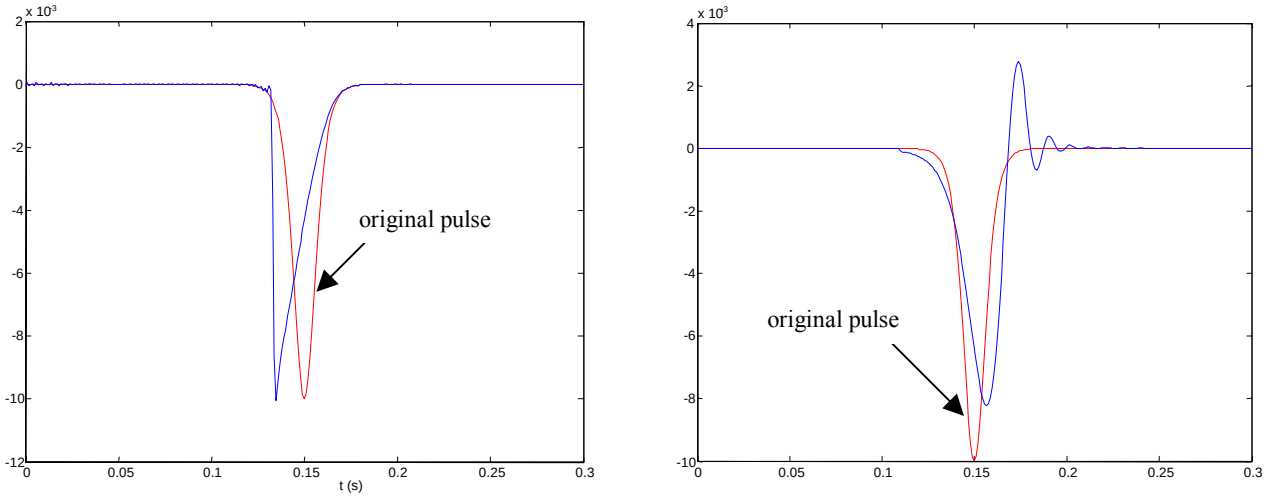

a) b)

Figure III.1 - Pulse profile achieved with a) nonlinear effects only

b) dispersion effects only

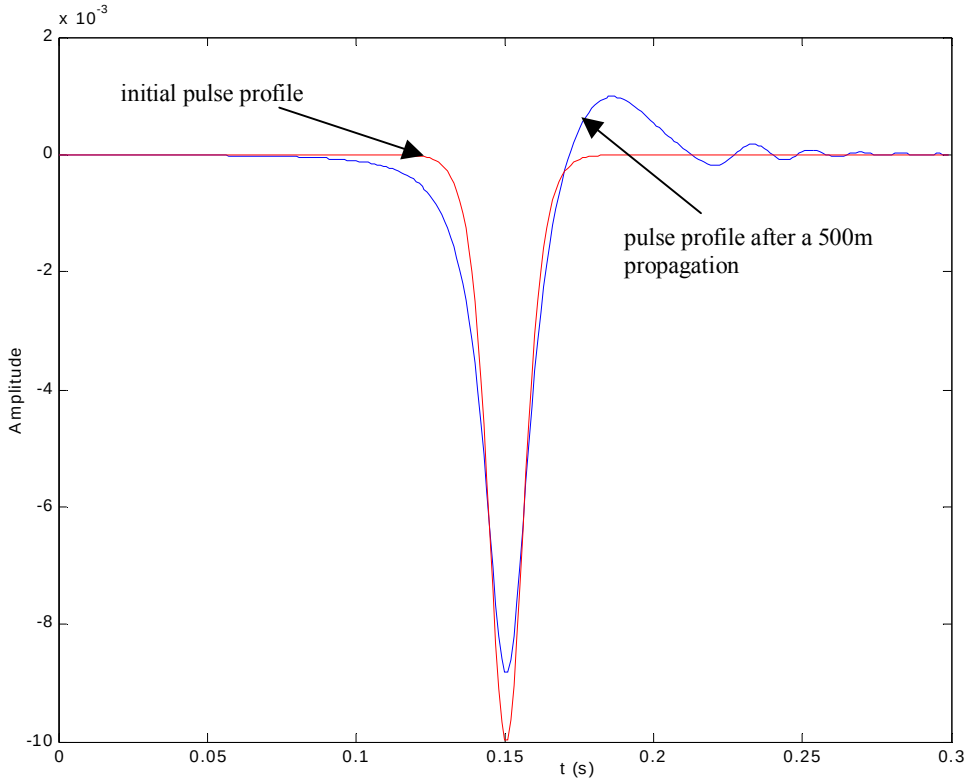

Figure III.2 - Propagation of a soliton

III.3. Initialization of the model

The simulation of the nonlinear propagation requires several inputs related to the signal generated by the transducer and to the properties of the nonlinear material in which the parametric amplification is obtained. The medium considered in this investigation is a mixture of castor oil and microspheres similar to that investigated by Herve Pincon [5] and Olivier Pauly [6].

III.3.1. Inputs related to the initial signal

The surface velocity of the source is inferred from the acoustic pressure, produced at 1m from the transducer, computed from its Transmitting Voltage Response (TVR) in water, and corrected for spherical spreading from the surface of the source. It is assumed for this calculation, that the particle velocity at the surface of the transducer does not depend on the surrounding medium since the mechanical impedance of the transducer is large and dominates the impedance of the surrounding medium. Therefore the particle velocity at the surface of the transducer is completely determined by the driving voltage.

The maximum driving voltage of the USRD Type-F56 transducer is $1000V_{rms}$ or a peak voltage of 1414 V. If each primary is driven with a peak voltage of 707 V the maximum allowed voltage will occur when the two primary signals are in phase with each other. The frequency of each primary is set as close as possible to the resonance of the transducer located at 13.1 kHz (see the TVR of the USRD TypeF56 transducer in the

Appendix B). This establishes the maximum voltage drive levels that could be used to generate the difference frequency, and thus the maximum enhancement that the nonlinear source could provide above that generated by the same transducer driven linearly at the difference frequency.

As an example of the calculation of the surface velocity, assume the difference frequency is 300 Hz; then the TVR of both primaries (respectively located at 12.9 and 13.2 kHz) equals 147.3 dB re 1 μPa/V. The sound pressure level generated by the transducer driven at a voltage V_T is related to the acoustic pressure at 1m of the source as follows:

$$P_0 = V_T * P_{ref} * 10^{\frac{TVR}{20}} \tag{III.14}$$

where P_{ref} represents the reference pressure (1μPa in water) and TVR refers to the Transmitting Voltage Response of the transducer. Therefore the corresponding acoustic pressure P_0 equals 3977Pa for a driving voltage of 182.5V at 1m from the source. The surface velocity of a radially oscillating sphere is given by [12]:

$$v_s = \frac{P_0 . r . \sqrt{1 + (ka)^2}}{\rho c_0 ka^2} \tag{III.15}$$

where k is the wave number, r the distance from the source at which P_0 is measured, and a the radius of the source. The use of linear acoustic equations to evaluate the surface velocity is justified by the fact that the surface velocity is inferred from the transmitting voltage response given in water where the nonlinear effects are negligible.

The particle velocity at the surface of the transducer is given for this example by the relation:

$$v_s = 0.0376 * \sin(2\pi\omega_1 t) + 0.0376 * \sin(2\pi\omega_2 t) \qquad \text{(III.16)}$$

Thus, the initial signal introduced in the program is given as a series of amplitude coefficients G_k and H_k corresponding to each harmonic frequency in equation (III.3) as follows:

Sine amplitude components		Cosine amplitude components
$G_1 = 0$	⟵ 300Hz ⟶	$H_1 = 0$
$G_2 = 0$		$H_2 = 0$
⋮		⋮
$G_{42} = 0$		$H_{42} = 0$
$G_{43} = 0.0376$	⟵ 12.9kHz ⟶	$H_{43} = 0$
$G_{44} = 0.0376$	⟵ 13.2kHz ⟶	$H_{44} = 0$
$G_{45} = 0$		$H_{45} = 0$
⋮		⋮

III.3.2. Inputs related to the nonlinear medium

The simulation program requires inputs related to nonlinear medium such as its nonlinear parameter and sound speed. These properties are evaluated for pressures ranging from 15 to 140 kPa, using the measurements of Pincon and Pauly, and then introduced in the simulation program.

The amplitude of the nonlinear coefficient as a function of the pressure is determined from Figure III.3 and the following relation:

$$\beta = 1 + \rho_0 c_0 \left(\left. \frac{\partial c}{\partial P} \right|_T \right) \Bigg|_{\rho_0} \qquad \text{(III.17)}$$

Where the partial derivative of the sound speed with respect to the hydrostatic pressure is evaluated at a temperature $T = 25°C$ and ambient density $\rho_0 = 870$ kg.m^{-3}.

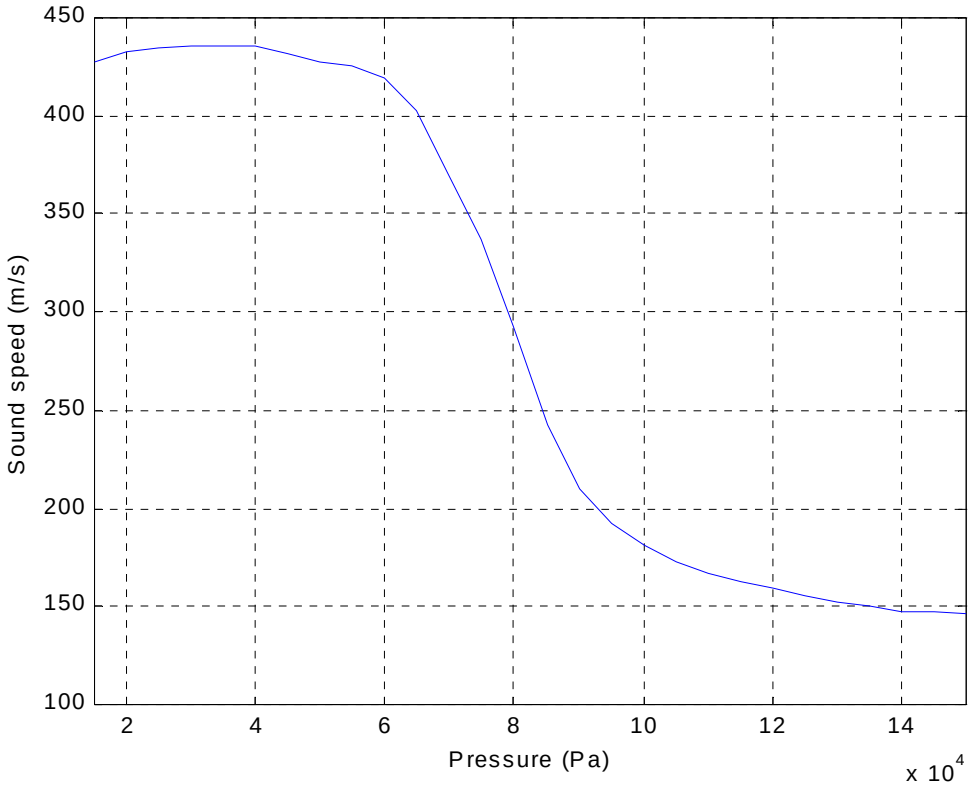

Figure III.3 - Sound speed dependence on the pressure at $25°\,C$

The values of the sound speed and the corresponding values of the nonlinear coefficients are listed in the following table for pressures ranging from 15 to 140kPa:

P (kPa)	15	20	25	30	35	40	45	50	55	60	65	70	75
C_0 (m/s)	428	433	435	436	436	436	432	428	425	419	406	370	333
β	370	371.6	94	1	1	-281	-185.4	-184	-460	-907	-2553	-2405	-2305

P (kPa)	80	85	90	95	100	105	110	115	120	125	130	135	140
C_0 (m/s)	293	243	210	193	181	173	166	163	160	155	153	150	148
β	-2535	-1366	-636	-375	-274	-186	-107	-71	-138	-66	-65	-64	-12

Table III.1- Values of the nonlinear parameter β and the sound speed c_0 for the medium castor oil-microspheres

III.4. Model predictions

III.4.1. Simulation of the nonlinear propagation

The simulation program was run for each of the pair of parameters $(c_0;\beta)$ in Table III.1 with primary frequencies located at 12.9kHz and 13.2kHz. The set of parameters, which produced the maximum difference frequency, was $(c_0;\beta)=(333;2305)$ and these conditions would be achieved by operating the transducer at a depth of 6.5m. The Figure III.4 depicts the normalized amplitude, corrected for the spreading loss, of the two primary frequency components and the difference frequency for this case of operation at a depth of 6.5m.

The correction for spreading loss, in Figure III.4, allows one to evaluate the nonlinear growth of the difference frequency and determine the distance beyond which the primaries cease to contribute to the growth. This distance determines the proper thickness of nonlinear material required to build the source. The amplitude of the difference frequency component grows immediately as a result of the nonlinear interaction of the primaries whose amplitude falls off as they distribute a large amount of energy to higher harmonics and especially to the sum frequency that shocks rapidly.

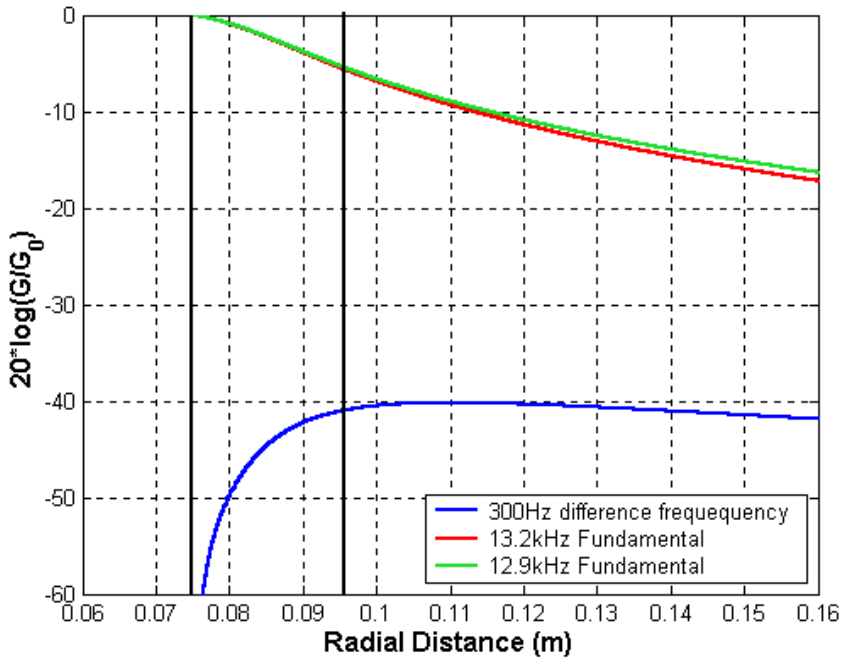

Figure III.4 - Amplitude of the particle velocity of the difference frequency and fundamentals

The thickness of the material layer is set equal to 2cm since the amplitude of the difference frequency reaches a maximum around 9.5cm from the center of the 7.5 cm radius transducer. The predicted sound pressure level generated for the difference frequency component at 1m from the source given a layer thickness of 2cm was 145.28dB ref 1μPa.

III.4.2. Contribution of the layer resonance

The large difference of impedance between the nonlinear medium and water results in a large reflected signal at the interface, which bounces back and forth between the rigid transducer and the high impedance fluid. The resonant amplification, resulting from the internal reflections, must be taken into account to evaluate the sound pressure level in the fluid outside the source.

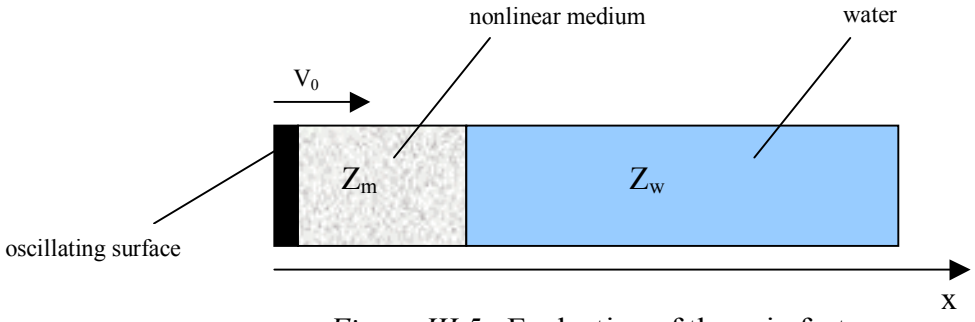

Figure III.5 - Evaluation of the gain factor

Assuming that the pressure varies harmonically, it can be expressed as:

$$p(x,t) = P(x)\exp(j\omega t) \tag{III.18}$$

Where $P(x)$ represents the pressure amplitude as a function of the distance to the piston, and ω the frequency of the signal considered.

Introducing $p(x,t)$ in the wave equation yields the Helmholtz equation, which has the solution:

$$P_T(x) = A * \exp(-jk_m x) + B * \exp(jk_m x) \tag{III.19}$$

Where k_m refers to the wave number of the signal of interest. The use of linear acoustic equations is justified by the fact that the difference frequency does not benefit from the nonlinear interactions on its way back to the transducer and during its successive reflections between the transducer and the boot. The solution consists of the superposition of waves traveling in the $+x$ direction (first term) and in the $-x$ direction (second term). Given the impedance of the nonlinear medium Z_m, the particle velocity can be expressed as:

$$U_T(x) = \frac{A}{Z_m}\exp(-jk_m x) - \frac{B}{Z_m}\exp(jk_m x) \tag{III.20}$$

The acoustic pressure transmitted into the water is of the same form as $P_T(x)$ except that it only consists of a wave traveling in the $+x$ direction since the surrounding medium is infinite. Therefore the acoustic field in water is expressed as:

$$P_W(x) = C_0 * \exp(-jk_w x) = C_1 * \exp(-jk_w(x-l))) \tag{III.21}$$

Where k_w refers to the wave number of the signal in water.

The corresponding particle velocity is expressed as:

$$V_W(x) = \frac{C_1}{Z_W} * \exp(-jk_w(x-l)) \tag{III.22}$$

The constant C_1 is to be determined from the boundary conditions to evaluate the amplification produced by the resonance in the layer of medium, and given by the relation:

$$\left|\frac{P(x=l)}{P(x=0)}\right| = \left|\frac{C_1}{V_0 Z_m}\right| \tag{III.23}$$

The continuity of the acoustic pressure and particle velocity at the interface medium-water provides the two first boundary conditions:

$$P_T(x=l) = P_W(x=l) \tag{III.24}$$

$$V_T(x=l) = V_W(x=l) \tag{III.25}$$

The third condition states that the particle velocity at $x = 0$ must equal the surface velocity V_0 of the transducer. These three conditions can also be reformulated as:

$$\begin{cases} A * \exp(-jk_m l) + B * \exp(jk_m l) = C_1 \\ A * \exp(-jk_m l) - B * \exp(jk_m l) = (Z_m / Z_w) * C_1 \\ A - B = V_0 Z_m \end{cases}$$

The amplification factor G is obtained by solving the system of equations for C_1 and is given by:

$$G = 20 * \log\left(\frac{1}{\sqrt{((Z_m / Z_w)\cos(k_m l))^2 + \sin^2(k_m l)}} \right) \qquad \text{(III.26)}$$

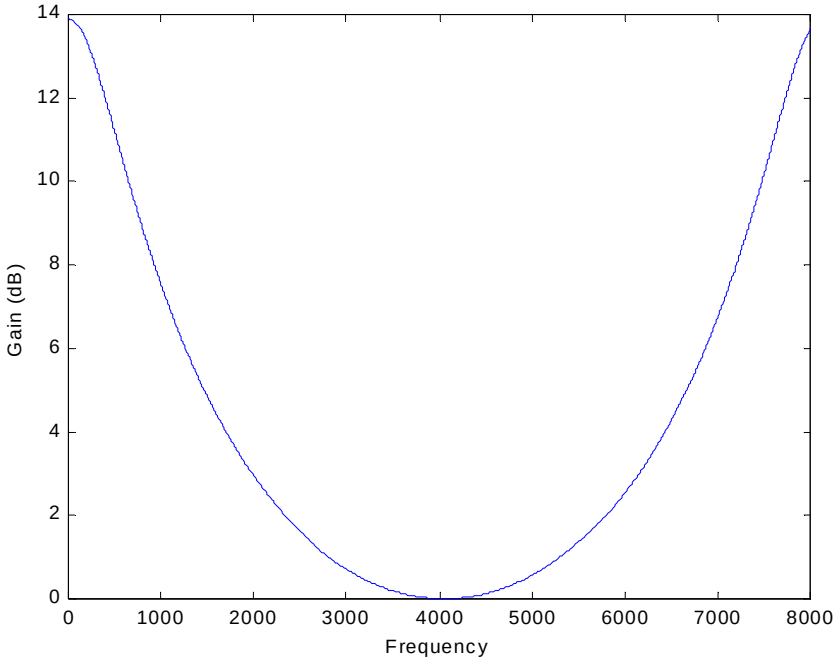

Figure III.6 - Gain factor as a function of the frequency

Thus, the result of the simulation program, given in the section III.4.1, needs to be corrected to account for the gain resulting from the layer resonance at the 300Hz difference frequency. The additional contribution, evaluated with Figure III.7, is 12.7dB. Therefore the theoretical prediction of the sound pressure level produced at the difference frequency is 158dB re 1μPa, when the transducer is driven with a peak voltage of 182.5 V at both primary frequencies.

III.4.3. Other model predictions

The simulation program was also used to investigate the optimization of the properties of the medium and of operation of the transducer.

The model predicts that when the primary frequencies are chosen closer to each other around the resonance of the transducer, the enhancement resulting from the nonlinear generation of the difference frequency component compared to what would be obtained driving the transducer linearly at the difference frequency increases. Thus, the advantage of the nonlinear source over the linearly operated source increases as the difference frequency decreases.

Dispersion was studied as a possible means to improve the parametric amplification. The destructive interactions resulting from dispersion between the generated harmonics, which are in phase with the fundamental and the freely propagating harmonics can result in inhibiting the growth of unwanted frequency components. However, these

interactions also affect generation of the difference frequency, due to the large downshift ratio, and impact the flow of energy back into the primaries from higher harmonics. The introduction of both small and large values levels of dispersion did not result in increasing the amplitude of the difference frequency component. Therefore introducing dispersion did not improve the efficiency of the nonlinear source and no physical mechanism to introduce dispersion was considered.

CHAPTER IV

EXPERIMENTAL IMPLEMENTATION

The model described in the previous chapter predicted a large enhancement in the difference frequency generation resulting from the addition of a layer of new nonlinear material to an omnidirectional source. This chapter presents an experimental realization of such a system.

IV.1. Preparation of a nonlinear medium

The nonlinear parameter *B/A* can be enhanced in media containing air bubbles either at frequency close to the resonance frequency of the bubbles (typically on the order of 1MGHz) thus inducing nonlinear oscillations, or at low frequency taking advantage of the dependence of the acoustic properties of the medium on the hydrostatic pressure.

While low difference frequency generation associated with ultrasonic parametric array in bubbly fluids, suffers from losses and practical difficulties, media whose properties

depend on hydrostatic pressure offer more flexibility for implementations of low frequency and therefore omni directional sources.

Large values of the parameter of nonlinearity can be achieved with media whose acoustic properties depend strongly on hydrostatic pressure. The nonlinear parameter β can be expressed as:

$$\beta = 1 + \rho_0 c_0 \left(\frac{\partial c}{\partial p} \right)_{T,\rho_0} + \frac{\beta_s T c_0}{c_p} \left(\frac{\partial c}{\partial T} \right)_{p,\rho_0} \qquad \text{(IV.1)}$$

and is determined for most media by the term proportional to $\left(\partial c / \partial p \right)$ since the dependence of the sound speed on the temperature is often negligible. The presence of microspheres in significant proportion in a medium implies a strong dependence of its compliance on the hydrostatic pressure and of its sound speed on the hydrostatic pressure – since sound speed and compliance are related.

Pincon [5] investigated a medium that consists of 90% Castor oil and 10% microspheres and reported a high negative value of the nonlinear parameter over certain pressure ranges (e.g. B/A=-2275 at a hydrostatic pressure of 35kPa). Although the medium Pincon investigated was highly nonlinear, it does not have the necessary properties for practical applications. In particular, the buoyancy of the microspheres requires a constant mixing to maintain a homogeneous mixture.

The implementation of an underwater source required a stable nonlinear medium and therefore the mixing issues related to the Castor Oil - Microspheres medium had to be eliminated. A homogeneous distribution of microspheres was obtained by mixing the microspheres in a gel just before it sets. The volume ratio of 1:10 of microspheres to host material was retained.

The gel is composed of water, salt, propylene glycol, Neodol® and Xanthan® gum (see Appendix C). Because of their small size (average radius of 30μm), the microspheres introduced in the gel are subjected to electrostatic forces and scatter very easily. Therefore it is necessary to spread the microspheres in water. The volume of microspheres mixed in water can be determined from the following relation:

$$V_m = \frac{m_{total} - \rho_w V_{total}}{\rho_m - \rho_w} \qquad \text{(IV.2)}$$

where m_{total} and V_{total} refer respectively to the mass and volume of the microsphere-water mixture, ρ_w is the density of water and ρ_m the density of the microspheres. A small excess of microspheres (11% instead of 10% of the total volume of medium prepared) is considered at the beginning of the each preparation to compensate for the loss resulting from the preparing of the medium.

The recipe of the Xanthan gel (Appendix C) provides the volume of each ingredient that needs to be added to an initial volume of water to obtain an approximately equal volume of gel. The initial volume of water was reduced by the change of volume resulting from adding the ingredients and by the volume already mixed with the microspheres to obtain the exact volume of gel required.

Mixing the gel with the microspheres tends to entrap free air bubbles and required the material to be placed in a vacuum chamber after each preparation. The nonlinear gel was evaluated as a practical nonlinear medium for a transducer application. The viscosity of the gel had to be sufficiently large to insure a fixed homogeneous distribution of the microspheres. A simple test was conducted by pouring a sample of medium into a beaker, and letting it stand for a long period after which the distribution of microspheres was examined and found to be unchanged.

It was also verified that a larger volume of medium obtained by adding up layers of gel-microspheres mixture provides a homogeneous medium and on which it is possible to pull a vacuum to eliminate all entrain air. The tests conducted showed that the medium is very easy to handle, however it should be noted that the gel must be covered when stored, to keep any surface in contact with the air from drying out.

IV.2. Preliminary measurements

The simulations given in the section III.4.1 used the nonlinear properties of the castor oil - microspheres medium. As explained in the section IV.1.1 only one of the terms that contribute to the nonlinear parameter is significant and the second term was shown for the medium castor oil microspheres to be equal to 0.59 whereas the term resulting from the dependence of the sound speed on the hydrostatic pressure equals –2275 at 35kPa.

The sound speed in the medium is related to the static bulk modulus as follows:

$$c = \sqrt{\frac{M_b}{\rho_0}} \tag{IV.3}$$

The bulk modulus relates the change of volume of a medium contained in a small pressure vessel (as measured by a scale on pump) to the corresponding change of pressure (displayed by the pressure meter) as follows:

$$\frac{1}{M_b} = -\frac{1}{V_0}.\frac{dV}{dP} \tag{IV.4}$$

Combining equations (IV.1) and (IV.3), shows that the nonlinear parameter is determined by the dependence of the bulk modulus on the hydrostatic pressure. Therefore the nonlinear parameter for the medium gel-microspheres was estimated by

comparing the dependence of the change of volume on the hydrostatic pressure for both media.

The bulk modulus measurement apparatus is shown schematically in Figure IV.1. The 216cm^3 pressure vessel is made of stainless steel (whose compliance is very low compared to that of the medium of interest). The change of volume was measured for hydrostatic pressures ranging from 0 to 117 kPa and the results are shown in Figure IV.2.

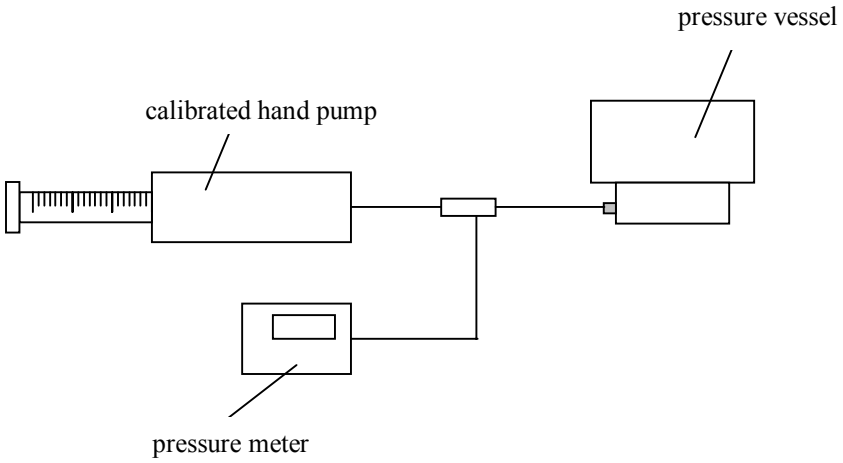

*Figure IV.1- M*easurement of the static bulk modulus of the nonlinear medium

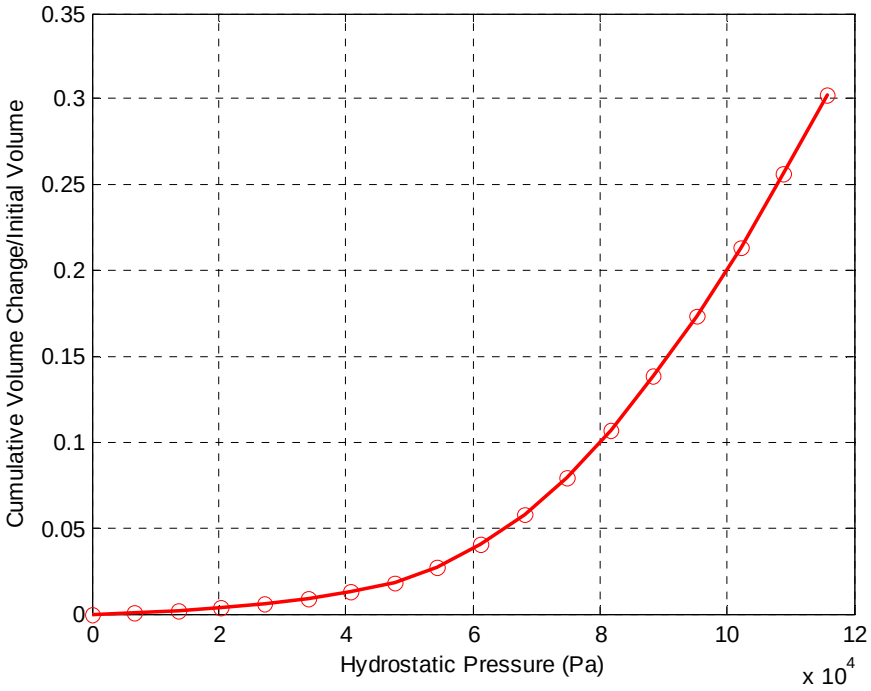

Figure IV.2 - Change of volume in the vessel as a function of the pressure

The graph exhibits three distinct regions of behaviors for the medium. For pressure values ranging from 0 to 34kPa, the bulk modulus is large (M_b=1.3e7Pa). This is because the microspheres behave as rigid entities at low pressures due to their hoop stiffness.

The amount of microspheres buckling in the medium progressively increases for values of the pressure ranging from 34 to 100 kPa, causing its compliance to increase and the bulk modulus to decrease. The pressure at which a microsphere buckles is determined by its geometry.

The buckling pressure of the microspheres modeled as thin spherical shells is given by Young [13] as:

$$P_{CR} = \frac{2E_s t^2}{r^2 \sqrt{3*\left(1-\sigma_s{}^2\right)}} \qquad \text{(IV.5)}$$

Where σ_s is the Poison ratio of the shell material and E_s is its Young modulus. r refers to the average radius of the sphere and t is the shell thickness. The properties of the microspheres used in the experiments are given below:

$$\sigma_s = 0.25$$
$$E_s = 3.15*10^9\, Pa$$
$$r = 30*10^{-6}\, m$$
$$t = 0.15*10^{-6}\, m$$

These properties yield a buckling pressure of 93.9kPa. This theoretical value is in consistent with the pressure of 100 kPa beyond which the change of volume in Figure IV.2 is linear. However the buckling pressure of most of the microspheres appears to be lower than the pressure computed above. This can be explained by the fact that the value of the radius used for the calculations is an estimate of the real value that seems in this case to be lower. Indeed, beyond this pressure, almost all the microspheres have buckled and start collapsing causing the medium to reach its maximum compliance. The largest value of the nonlinear parameter, which is proportional to the partial derivative

of the bulk modulus with respect to the hydrostatic pressure, corresponds to the pressure region for which the change of bulk modulus divided by the sound speed is the largest.

It is determined from the Figure IV.2 that the pressure corresponding to the largest nonlinear parameter is located at 62kPa, which corresponds to a depth in water of 6.5m where the measurements will be performed. The difference frequency generation is determined by the nonlinear parameter as well as by the sound speed of the medium. However since the sound speed in the medium was not measured over a range of hydrostatic pressures, the measurements will be performed at a depth in water of 6.6m corresponding to a hydrostatic pressure of 35kPa and giving the largest coefficient of nonlinearity.

IV.3. Construction of the source

IV.3.1. Description of the source

The source consists of a ceramic transducer (described in section IV.3.2) of outer radius 7.5cm encapsulated in a 2cm layer of the nonlinear medium and enclosed in a thin spherical boot (see Figure IV.3).

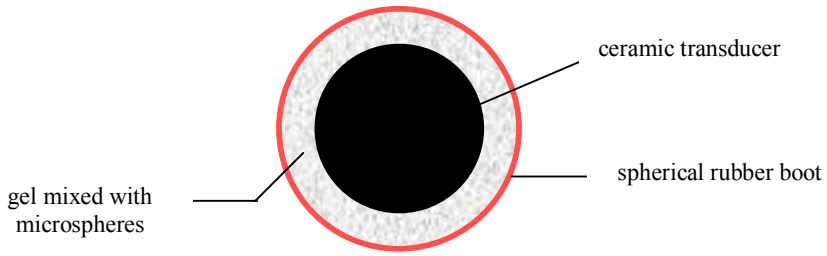

Figure IV.3 - Description of the source

The boot has to maintain certain dimensions and needs to be made of a material whose stiffness allows it to keep its shape when released. It must be thin enough and matched well enough in impedance so as not to impede the radiation of the difference frequency signal into the surrounding medium.

The proper thickness of the layer of nonlinear medium was estimated at 2cm according to the predictions of the third chapter, which implies an inner radius of the boot of 9.5cm. Its thickness is chosen equal to 3mm which is small enough to limit the

attenuation of the outgoing signal but sufficiently thick to insure a waterproof protection of the nonlinear medium and the transducer.

IV.3.2. Assembly of the transducer

The transducer referenced USRD F56 PZT-IV (see Appendix B) consists of two radially poled PZT ceramic hemispherical shells of external radius 7.5cm. The piezoelectric properties of the ceramic shell convert a difference of applied potential, between its inner and the outer surface, into a change of thickness.

Each element of the shell undergoes a thickness expansion (determined by the d_{33} coefficient of the piezoelectric tensor of the material) and a lateral expansion (determined by the d_{13} coefficient) proportional to the electric field applied through the thickness of the shell (see Figure IV.2) and which causes the displacement of its external surface.

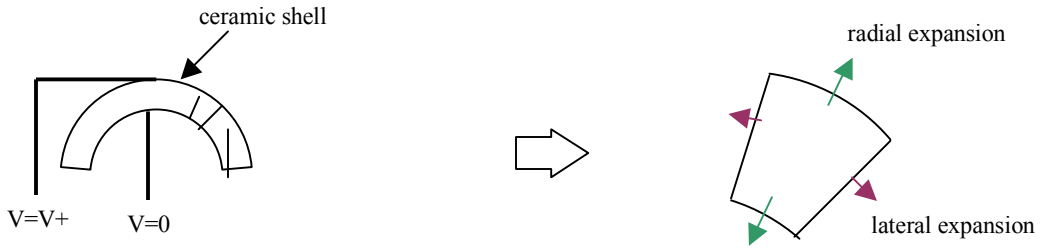

Figure IV.4 - Expansion undergone by a shell element

A hole is filed in each hemisphere to allow the wire to connect the interior surface of the two hemispheres and provide continuity. The two hemispherical parts of the transducer are assembled and connected as shown in Figure IV.5.

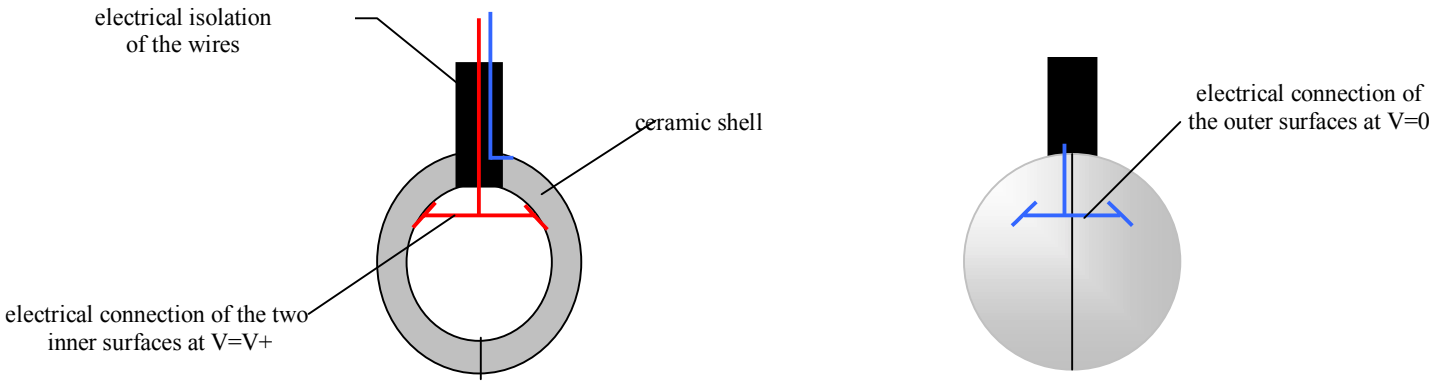

Figure IV.5 - Assembling and electrical connections of the transducer

a) Cross section b) Front view

A brass bolt with the threading pointing upward, goes through the hole filed in the hemisphere, connects the two interior surfaces and is isolated from the external surfaces of the transducer. Since the rubber boot was too soft to support the weight of the source, a small rod was screwed on the threading of the bolt and was used as a support (see Figure IV.6).

Figure IV.6 - Assembled transducer

IV.3.3. Design and construction of the mold

The mold, in which the two parts of the boot were cast, consists a hemispheric concave mold of radius 9.8cm made of plaster and a sphere of radius 9.5cm. The plaster mold was obtained by immersing half of a sphere of external radius 9.8cm in a mix of Plaster of Paris® and water before it cured (see Figure IV.7 and Figure IV.8).

Since no sphere of radius 9.8cm was found available, a medicine ball of radius 9.5 was bought and several pieces were cut in a soft material of thickness 3mm and stuck to the ball to obtain a hemisphere with the proper radius. The gaps between the pieces were then filled with molding clay to achieve the smoothest surface as possible and a thin layer of cellophane is applied on the ball as a sealant.

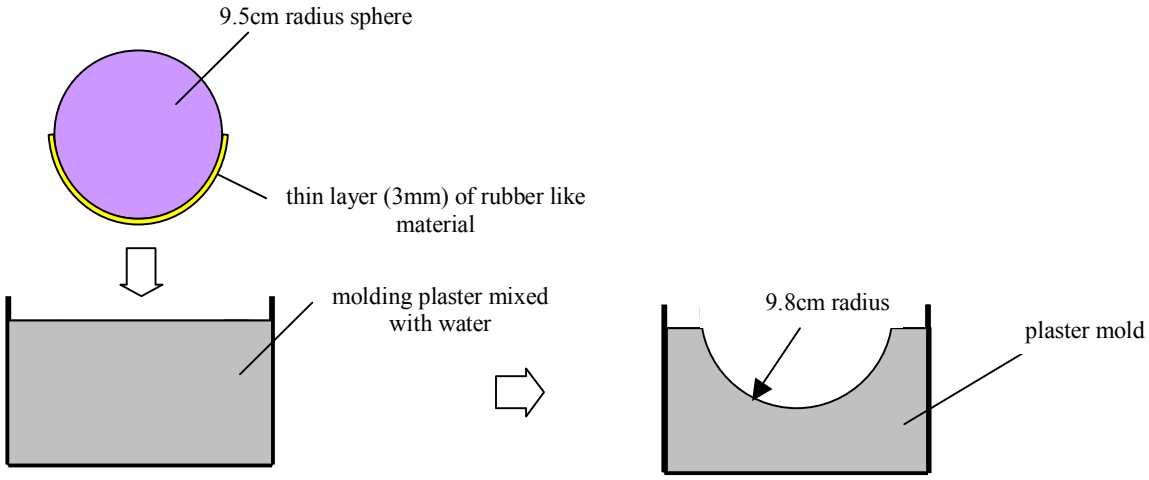

Figure IV.7 - Casting of the plaster mold

Figure IV.8 - Plaster mold

IV.3.4. Design of the boot

Once the plaster mold had cured, its concave hemispherical surface was smoothed and sealed to facilitate the casting of the rubber. The choice of the polyurethane used to realize the boot was motivated by its low stiffness (hardness shore A = 40) and by the fact that its low viscosity reduces bubbles entrapment as it cures. A vacuum was pulled on the polyurethane before to pour it into the mold to guaranty a completely bubble free rubber boot.

The ball, from which the layer of rubber like material was first removed, was stuck to a structure that maintains a spacing of 3mm between the ball and the plaster mold. The liquid rubber (polyurethane) was then poured into the mold; the ball was introduced and the material allowed curing overnight in an oven set at 90F. This part of the procedure is illustrated in Figure IV.9.

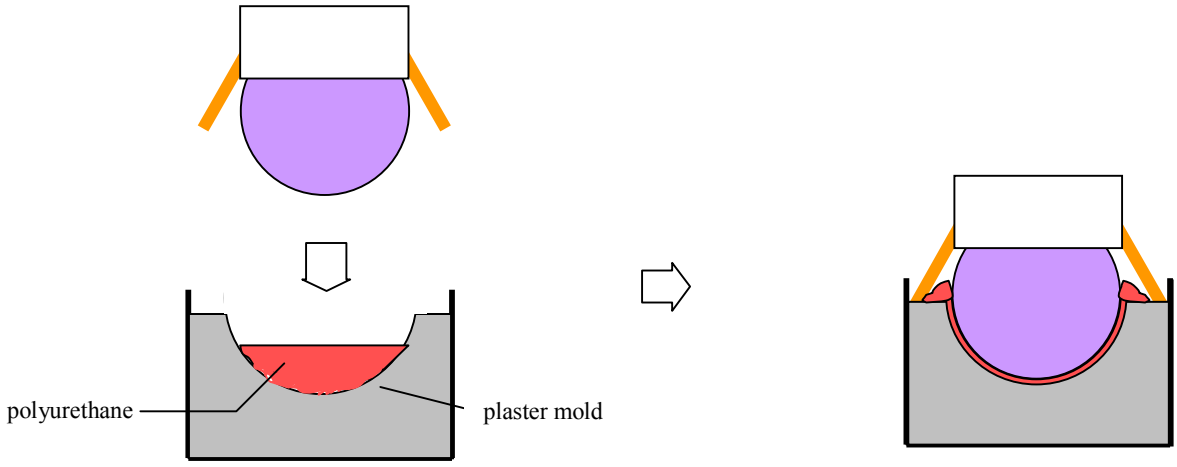

Figure IV.9 - Casting of the rubber boot

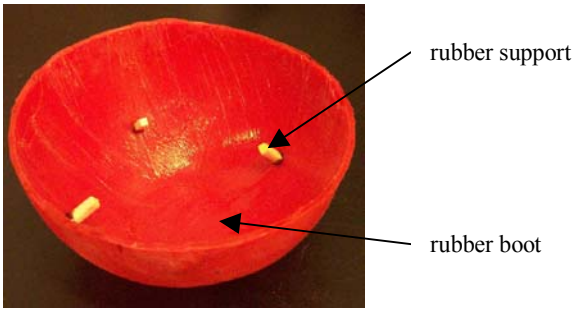

Figure IV.10 - Hemispheric rubber boot

After the curing, four supports of length equal to the thickness of the layer of nonlinear material were stuck on the inside surface of the boot (see Figure IV.10) with polyurethane glue to insure a constant spacing between the boot and the transducer when assembled.

Although the two parts of the rubber boot had been cast separately, their edges had to be complementary to facilitate assembly. The medicine ball was covered with these hemispheres and the gap was filled with the polyurethane rubber. After the curing, the shell made of the two hemispheres was cut on its equator to obtain two complementary parts.

IV.3.5. Assembly of the source

Several layers of gel were sequentially poured into the lower half of the rubber boot, which was supported by the plaster mold. Each batch of material introduced was evacuated before pouring. The PZT transducer was then hung 2cm off the bottom of the mold by a wire with the rubber supports within the boot helping to maintain the proper spacing between the boot and the transducer (see Figure IV.11).

Entrapment of air bubbles resulting from placing the transducer in the gel was reduced by spraying water on the surface of the gel and slowly sliding the bottom of the transducer into contact with the gel, allowing air bubbles to rise out of the contact surface.

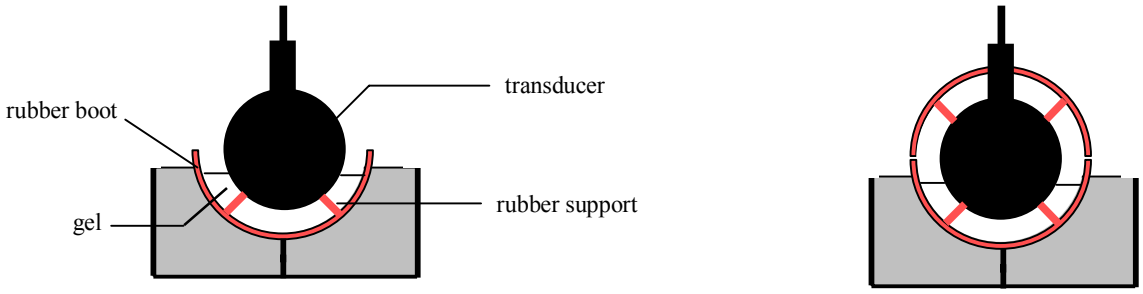

Figure IV.11 - Assembly of the source

A hole was cut on the top of the upper hemisphere to allow the electrical wires of the transducer to pass through (see Figure IV.12). The upper hemisphere was then stuck to

the lower one with a soft polyurethane glue. The same glue was used afterwards to cover the equator of the boot and provide a waterproof gluing between the two parts.

The remainder of the medium was injected from the top of the upper hemisphere below the surface of the gel to eliminate the introduction of air.

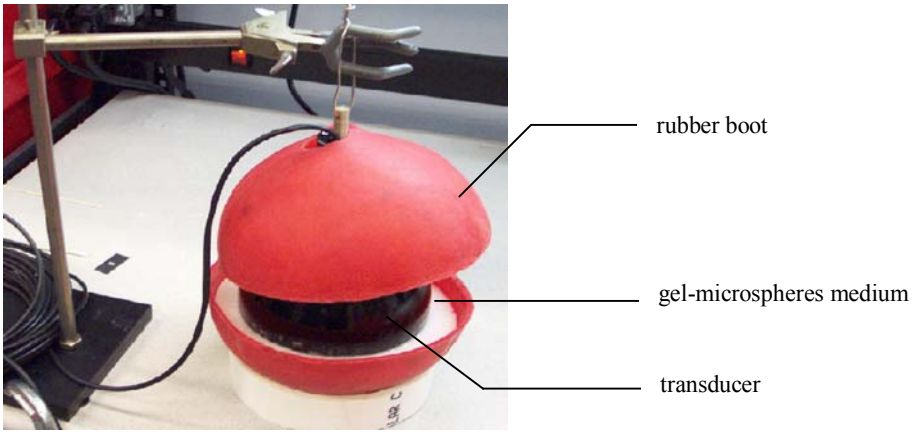

Figure IV.12 - Source with medium in the bottom half of the boot

When the upper part of the source was almost filled, the remaining nonlinear medium needed to fill the space between the boot and transducer was carefully introduced with a syringe.

The system was sealed by gluing top of the rubber boot to the cylinder of polyurethane used to isolate the electrical connections of the transducer from the surrounding water. The completed source is shown in Figure IV.13.

Figure IV.13 - Completed source

CHAPTER V

MEASUREMENTS

The transducer was tested in the acoustic tank facility at Georgia Tech. The experimentally measured sound pressure level of the difference frequency component is compared both with model predictions and with sound pressure level values that would result from driving the transducer linearly. This chapter describes the experiment and presents and analyses the results. . The first section describes the experimental setup; the second section contains the presentation and analysis of results and the last section is devoted to error analysis.

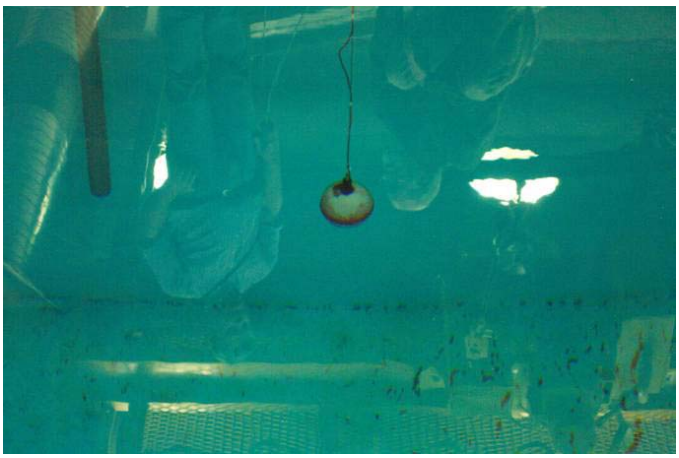

Figure V.1 - Source submerged in the water tank

V.1. Experimental setup

V.1.1. Positioning of the source

The analysis of the static modulus predicted that the nonlinear parameter required to achieve the largest parametric amplification would occur at a hydrostatic pressure of 65 kPa. The source was lowered in a water tank to a depth of 6.6m, where the source is subjected to the required hydrostatic pressure. The transducer was hung by a steel cable whose length was used to determine the depth of the transducer (see Figure V.2).

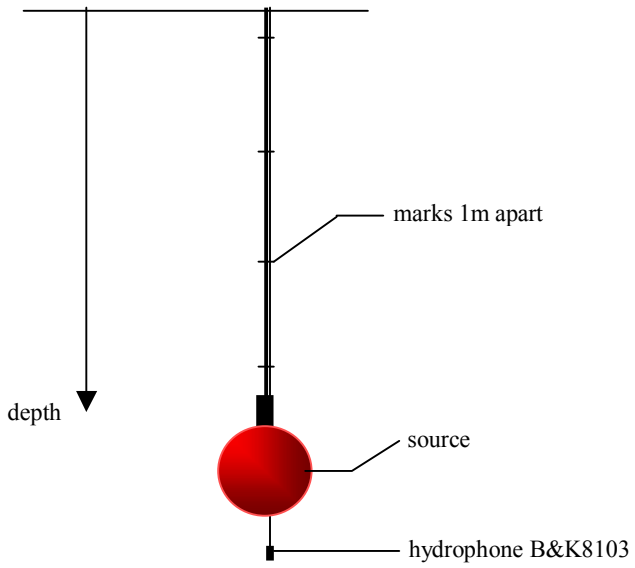

Figure V.2 - Experimental setup

V.1.2. Driving voltage applied to the transducer

The voltage applied to the transducer was produced by a function generator (Polynomial waveform synthesizer Analogic® Model 2020) and amplified (Instrument Inc.® Model 16) with a gain of 10^3. As an example, the driving waveform shown in Figure V.3 was obtained with the input voltage at the function generator set to

$$V(t) = 0.182 * \sin(12.9k * t + 0.5) + 0.182 * \sin(13.2k * t) \qquad \text{(V.1)}$$

and resulted in an actual driving voltage of 180V for each primary. The first term, which represents one of the fundamentals, was slightly time shifted to make the waveform start at zero, in order to avoid transient effects. The voltage monitoring output (which gives the actual amplified voltage/100) of the amplifier was connected to an oscilloscope to display and record the waveform corresponding to the driving voltage.

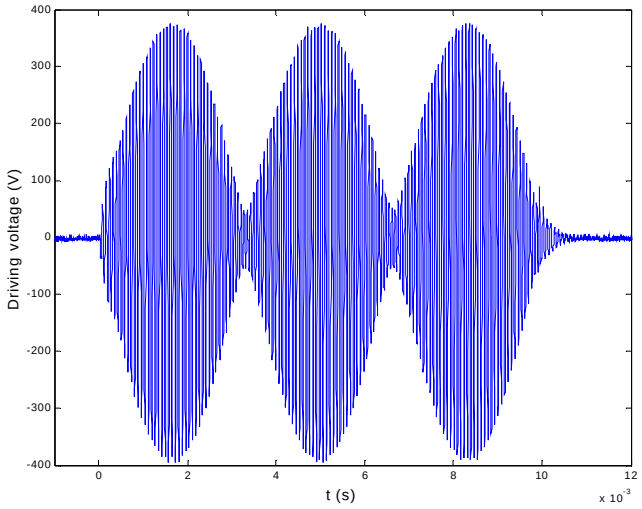

Figure V.3 - Driving voltage applied to the transducer

The beating phenomenon in the waveform of Figure V.3 results from the interference of two sinusoidal signals with frequencies close to each other.

V.1.3. Data acquisition

The acoustic pressure was measured with two B&K model 8103 hydrophones, (see Appendix D) which have a 6m low noise shielded cable and which can operate over a frequency range from 0.1Hz to 180kHz. Although a single hydrophone would have been sufficient to perform the measurements, a second one was used, in case the first one did not work correctly. The hydrophones were connected to the preamplifier (SRS® model SR560) using a relatively long cable whose capacitance reduced the overall sensitivity. The loss of sensitivity can be computed with the following relation:

$$L_\sigma = 20 * \log\left(\frac{C_{HYDRO}}{C_{HYDRO} + C_{CABLE}}\right) \qquad \text{(V.2)}$$

where L_σ represents the loss of sensitivity in dB, C_{HYDRO} the capacitance of the hydrophone measured at the end of its cable, and C_{CABLE} the capacitance of the cable that connects the hydrophone to the preamplifier. The value of the capacitance of the hydrophone with its cable is equal to 3620pF and the capacitance of the added cable equals 740pF. The resulting sensitivity loss equals 1.6dB, which has to be added to the sound pressure level evaluated from the measured signal.

Since the source is omnidirectional the hydrophones can be positioned anywhere relative to the source. The source, located at 6.5m from the surface, was close to the bottom of the tank. Therefore, the hydrophones were positioned above the source to limit the detection of signals reflected from the bottom of the tank. The measured signal was amplified with a gain of 10, bandpass filtered between 100Hz and 30kHz, and displayed on an oscilloscope. The signal was recorded digitally for post-experiment signal processing.

V.2. Processing of the data

The waveform at the output of the hydrophones is a voltage signal that has to be converted into a pressure signal. In order to compute the source level (which is defined as the pressure referred to a distance 1 meter from the source), the signal is first divided by the gain factor of the preamplifier and the sensitivity of the hydrophone ($\sigma = 24.8\mu V / Pa$) and then multiplied by the distance that separates the hydrophones from the source. The resulting pressure waveform is shown on Figure V.4.

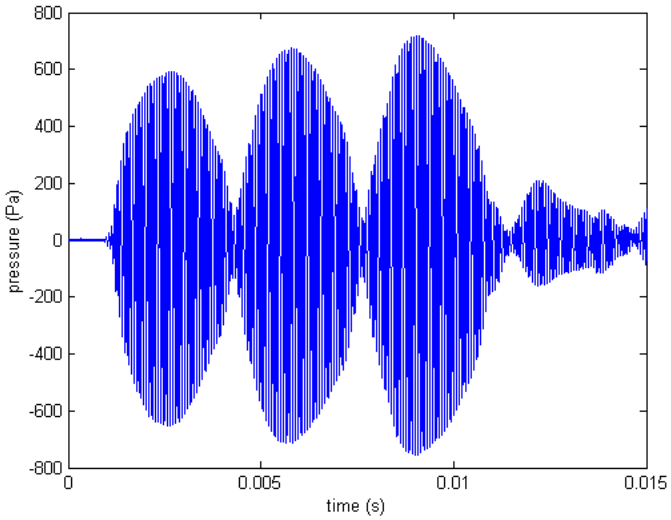

Figure V.4 - Signal radiated by the source at a depth of 6.5m (referred to 1 m)

The signal shown in Figure V.4 includes all frequency components between 100Hz and 30kHz, radiated by the source. The waveform corresponding to the difference

frequency components needs to be extracted and compared to the amplitude predicted by the model.

V.2.1. Filtering of the signal

A Butterworth low-pass filter of the third order is applied to the waveform to eliminate the amplitude of the primaries and their harmonics and retain the difference frequency part of the waveform. The order of the filter determines the sharpness of the frequency window outside from which the frequency content of the signal is eliminated. The cutoff frequency of the filter is arbitrarily chosen to be 2000Hz.

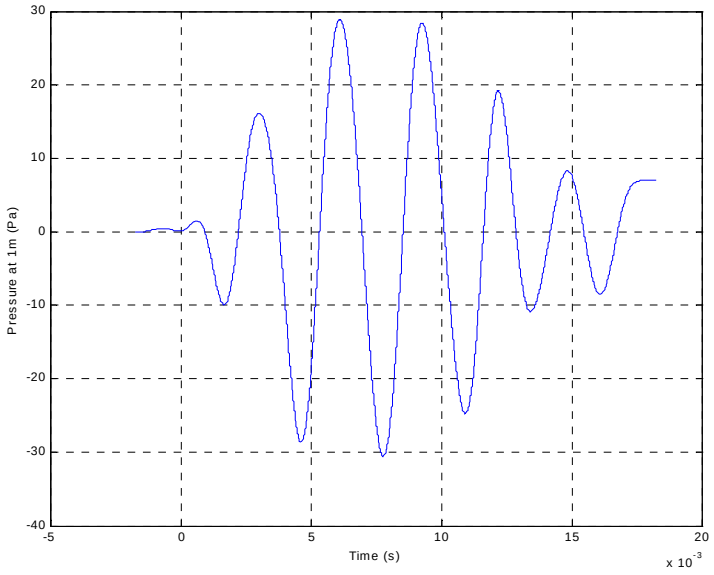

Figure V.5 - Difference frequency waveform at a depth of 6.5m

V.2.2. Evaluation of the sound pressure level

The sound pressure level corresponding to the difference frequency component at 1m from the source is inferred from the peak pressure value of the difference frequency waveform measured from Figure V.5, using the relation

$$SPL = 20 * \log\left(\frac{P}{P_{ref}}\right) \qquad \text{(V.3)}$$

Where the reference pressure, P_{ref} is 1 μPa. The acoustic pressure P reaches a maximum of 30.5 Pa and yields a sound pressure level of 149.7dB. Accounting for the various corrections discussed in IV.1, the actual sound pressure level at 1m from the source is 151.3dB.

V.2.3. Enhancement of the sound pressure level

The transmitting voltage response of the transducer F56 is given for frequencies ranging from 1kHz to 15kHz. However, assuming that the TVR curve can be extrapolated to frequencies below 1kHz, the sound pressure level obtained by operating the transducer at 300Hz with a driving voltage of 365V is inferred from relation IV.14. The TVR at 300Hz is estimated at 82.6dB/V re 1μPa which would yield a sound pressure level of 134 dB at 1m from the transducer. Therefore the low frequency sound produced

parametrically was 17dB higher than could have been obtained by driving the transducer element directly at the difference frequency with the same peak voltage.

V.2.4. Comparison with the model prediction

The model predicts a sound pressure level of 158 dB for the difference frequency, which is 7dB higher than what was actually measured. There are a number of factors, which could contribute to this discrepancy.

Several uncertainties related to the experimental apparatus may alter the measurements:

(1) The preamplifier (SR560) has a gain accuracy of 1% between DC and 10kHz and 3% between 10kHz and 100kHz.

(2) The sensitivity of the hydrophone B&K8103 can vary from 22 to 38μV/Pa (see Appendix D)

(3) During its successive reflections inside the layer, the amplitude of the difference frequency signal is reduced by the attenuation processes. Therefore, the effect of the layer as calculated in the model may be larger than it really is.

As the source is lowered at 6.5 m, it is subjected to a hydrostatic pressure of 65kPa that compresses the layer of nonlinear medium and reduces its thickness. The corresponding

change of volume can be evaluated from the static measurements for the medium gel microspheres in the section IV.2. The initial volume of medium introduced in the source is 1.82 L and the cumulative change of volume /volume initial equals 5% at 65kPa that yields a change of volume of 9.1 mL and a change of thickness of 1mm. The amplitude of the particle velocity corresponding to the difference frequency component at 1.9cm from the transducer is very close to particle velocity at 2cm. The effect of the change of thickness on the layer resonance contribution is also very small.

(4) The actual sound pressure level of the ceramic may be different from the sound pressure level deduced from its TVR at 300Hz and could only be determined by performing measurements with the transducer immersed in water.

(5) The properties of the medium introduced in the numerical model are not precisely known and the results provided by the simulations may therefore have uncertainties.

(6) The distance from the source at which the hydrophones were positioned may have not been measured precisely.

CHAPTER VI

CONCLUSION

VI.1. Summary of the work

A compact, omnidirectional, parametric source has been designed and tested. Preliminary results indicate a significant enhancement of the sound pressure level for the difference frequency component relative to that obtained when driven linearly at the difference frequency. The parametric amplification was theoretically estimated with a numerical model modified to take into account the dispersion effects.

The dispersion effects introduced in the model were observed to have no impact on the parametric amplification. Indeed, they reduced the amplitude of the harmonics as well as the primaries themselves, without resulting in any increase in the difference frequency component

The validation of the program was followed by the running of simulations to estimate the level of difference frequency generated due to the presence of a layer of a highly nonlinear material as a function of hydrostatic pressure.

The largest amplification was achieved at a hydrostatic pressure of 65kPa for which the nonlinear parameter (β=2305) combined with a small sound speed (c_0=333m/s) generates the highest level of difference frequency. The numerical results were used to determine the thickness of material required to optimize the parametric amplification. The optimal thickness was found to be 2cm.

The nonlinear properties of the medium, used the simulation program, were then compared to those of a nonlinear medium suitable for practical implementations, and found to be similar. The transducer was built according to the model specifications. The design process included: (1) the preparation of the nonlinear medium consisting in a mix of gel with microspheres; (2) the construction of a thin spherical rubber boot used as a shell inside which the transducer was surrounded by the gel; and (3) the assembling of the source.

An experiment was conducted with the source to measure the parametric amplification of the difference frequency component resulting from the layer of nonlinear medium. The measurements were performed in a water tank where the source was lowered at

6.6m and subjected to a pressure of 65kPa. Experimental results were compared to the prediction from the numerical model and a good agreement was found.

VI.2. Results

The sound pressure level generated nonlinearly was observed to be 17dB above that which would be obtained by driving the source linearly at the difference frequency. The discrepancy between the theory and the experiment is approximately 7dB, which is reasonably small, and indicates that the modeling of the source was reasonable. However, there are several possible reasons that may explain this discrepancy. The main identified source of discrepancy is the fact that linear attenuation was not taken into account to evaluate the contribution of the layer resonance.

VI.3. Future work

A new system is currently under construction to precisely position the hydrophones to limit the reverberation effects due to the fact that the source was located close to the bottom during the measurements reported here.

The presence of the layer of nonlinear medium improved the sound pressure level of the difference frequency component by 17dB. However, most of the primaries energy is lost

generating the sum frequency component and other harmonics, and the parametric amplification of the difference frequency would incontestably benefit from limiting the growth of these unwanted frequency components.

Rogers and Van Buren [14] envisioned a parametric source fitted with a pressure release reflector end causing the harmonic components to reflect with a phase shift of 180 degrees and destructively interact on their way back to the transducer with incident harmonics. A pressure release reflector end used on the constructed source may help to save energy for the amplification of the difference frequency component.

APPENDIX A

SIMULATION PROGRAM

```
% Initialization of the variables

J=3000;                                 % Number of harmonics
g(1:J)=0.0000000000;                    % Gk coefficients
g(12)=0.150273;
g(13)=0.16781;
gx(1:J)=0.0000000000;
g2(1:J)=0.0000000000;
h(1:J)=0.0000000000;                    % Hk coefficients
hx(1:J)=0.0000000000;
h2(1:J)=0.0000000000;
x1(1:J,1:J)=0.0000000000;
x11(1:J,1:J)=0.0000000000;
x2(1:J,1:J)=0.0000000000;
x22(1:J,1:J)=0.0000000000;
freq=1000;                              % Difference frequency
c=370.000;                              % Sound speed in the medium
beta=-1300.0;                           % Coefficient of nonlinearity
e=1;                                    % Normalization coefficient
dx=0.00625;                             % Stepsize
ro=0.075;                               % Starting distance
deltaC=0;                               % Sound speed step
coef=400;                               % Number of harmonics reduced
k=2;                                    % Number of initial coefficients
ki=0;

% Computation of the absorption coefficients

alpha(1)=0.03;
for i=2:J
    alpha(i)=i*i*alpha(1);
end

% Computation of the dispersion coefficients

for i=1:J
    delt(i)=(i*freq*2*pi/c)*(1-(c/(c+(i-1)*deltaC)));
end
```

```
% Compute the matrix element

b=pi*beta*freq/(c*c);

for id=2:J
    izx=id-1;
    for im=1:izx;
        x11(id,im)=exp((alpha(id)-alpha(im)-alpha(id-im))*dx);
        x1(id,im)=1.00000;
        end
end
ifx=J-1;
for inn=1:ifx
    inz=J-inn;
    for ip=1:inz;
        x22(inn,ip)=exp((alpha(inn)-alpha(ip)-alpha(inn+ip))*dx);
        x2(inn,ip)=1.00000;
        end
end
gh(1:J)=exp(-alpha(1:J)*dx);
rn=r0;
r=rn;
f1=1.000000000;
a=1;


for iii=1:2000                      % iii = number of steps
r=ro+iii*dx;                        % propagation distance
cb=dx*b*f1;
g2(1:J)=g(1:J);
h2(1:J)=h(1:J);
dg(1:J)=0.0000;
dh(1:J)=0.0000;
dg1(1:J)=0.0000;
dh1(1:J)=0.0000;

% Computation of the first derivative

    for is=2:J
        ill=is-1;
        for it=1:ill
        cx=cb*it*x1(is,it);
        dg(is)=cx*(g2(is-it)*g2(it)-h2(is-it)*h2(it))+dg(is);
        dh(is)=cx*(h2(is-it)*g2(it)+g2(is-it)*h2(it))+dh(is);
        end
    end
    for iu=1:J
        izz=J-iu;
        for iv=1:izz
        cx=cb*iu*x2(iu,iv);
        dg(iu)=dg(iu)-cx*(g2(iu+iv)*g2(iv)+h2(iu+iv)*h2(iv));
```

```
        dh(iu)=dh(iu)+cx*(g2(iu+iv)*h2(iv)-h2(iu+iv)*g2(iv));
        end
    end

% Computation of the new amplitudes for the second derivative

g2(1:J)=g(1:J)+dg(1:J);
h2(1:J)=h(1:J)+dh(1:J);

ii=J-coef;

g2(ii:J)=0.8*g2(ii-1);              % Reduction of the last harmonics
h2(ii:J)=0.8*h2(ii-1);              % Reduction of the last harmonics
r=r+dx;
f1=rn/r;
cb=dx*b*f1;

% Computation of the second derivative

    for is=2:J
        ill=is-1;
        for it=1:ill
        cx=cb*it*x11(is,it);
        dg1(is)=cx*(g2(is-it)*g2(it)-h2(is-it)*h2(it))+dg1(is);
        dh1(is)=cx*(h2(is-it)*g2(it)+g2(is-it)*h2(it))+dh1(is);
        end
    end
    for iu=1:J
        izz=J-iu;
        for iv=1:izz
        cx=cb*iu*x22(iu,iv);
        dg1(iu)=dg1(iu)-cx*(g2(iu+iv)*g2(iv)+h2(iu+iv)*h2(iv));
        dh1(iu)=dh1(iu)+cx*(g2(iu+iv)*h2(iv)-h2(iu+iv)*g2(iv));
        end
    end

% Computation of the new amplitudes.

g(1:J)=g(1:J)+0.5*(dg(1:J)+dg1(1:J));
h(1:J)=h(1:J)+0.5*(dh(1:J)+dh1(1:J));

g(ii:J)=0.8*g(ii-1);                % Reduction of the last harmonics
h(ii:J)=0.8*h(ii-1);                % Reduction of the last harmonics

for ix=1:J
        g(ix)=g(ix)*f1*gh(ix);
        h(ix)=h(ix)*f1*gh(ix);
end

% Introduction of the dispersion

for i=1:J
    a1=g(i);
```

```
    b1=h(i);
    c1=delt(i);
    g(i)=(a1*cos(c1*dx)+b1*sin(c1*dx));
    h(i)=(b1*cos(c1*dx)-a1*sin(c1*dx));
end
    rn=r;
    r
    g(1)
    se=[];
    fido=fopen('fundamental.txt','w');
    fprintf(fido,'%f ',g);
    fprintf(fido,'\n',se);
    fclose(fido);

% Recording of the coefficients in text files

    if (mod(iii,10)==0)
        fid1=fopen('CosNumEnd.txt','w');
        fid2=fopen('SinNumEnd.txt','w');
        for (i=1:J)
        fprintf(fid1,'%1.10f\n',h(i));
        fprintf(fid2,'%1.10f\n',g(i));
        end
        fprintf(fid1,'%1.10f\n',r);
        fprintf(fid2,'%1.10f\n',r);
   st1=fclose(fid1);
   st2=fclose(fid2);
    end

end
```

APPENDIX B

TRANSDUCER USRD F-56

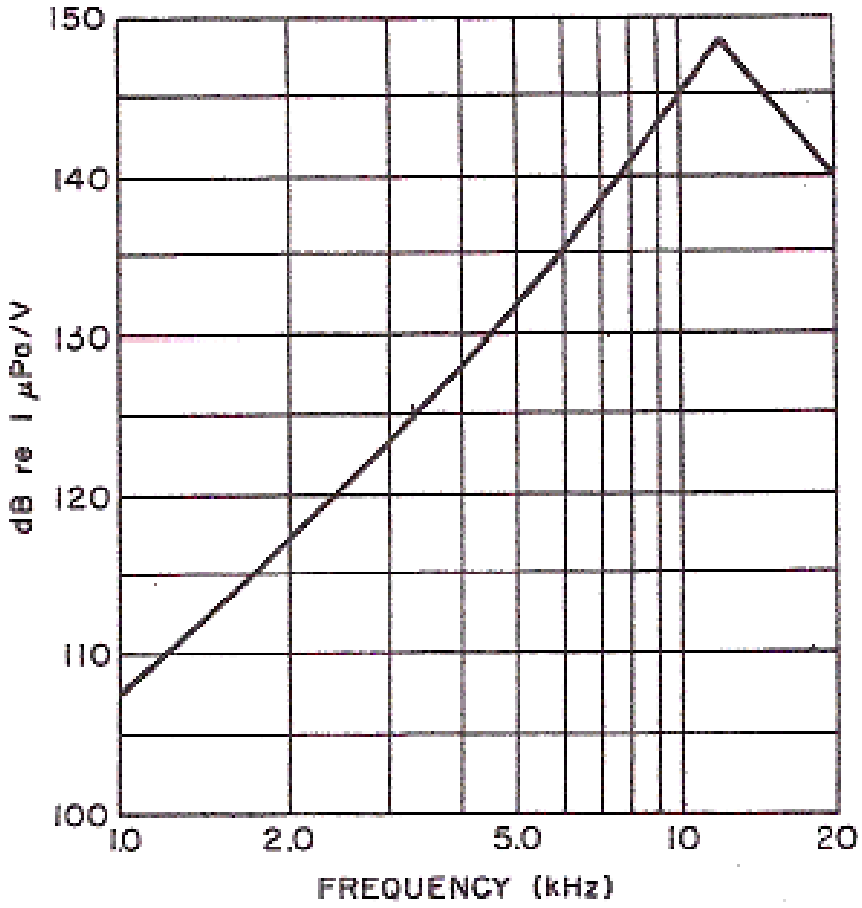

Typical Transmitting Voltage Response for

Type F56 transducer

APPENDIX C

XANTHAN GEL RECIPE

To make about 1L of polymer stabilized bubble cloud:

1- In a beaker, dissolve 35g of salt into about 1L of air saturated water at room temperature

2- In a separate beaker, pour in 30g of propylene glycol (the dispersant, we need this because Xanthan gum is no water soluble). To the glycol…

   - add 5g of Neodol (a surfactant) then…
   - add 10g of Xanthan gum (the polymer, use Keltrol BT)
   - stir but do not let stand too long before mixing with the saline solution (step3). It will settle and can affect its properties if it is not used for a long time.

3- Pour the xanthan gum mixture into the salt water while stirring. Continue stirring until the mixture looks fairly uniform. (We may need to buy a large stirring rod).

4- Let stand. After about 1 hour, you will have a bubbe cloud about .1%-.3% void fraction, assuming that the water was initially saturated with air.

Larger or smaller quantities can be made by maintaining proportions. Also, care must be taken while stirring in order to avoid entraining bubbles.

P.A. Hwang, R.A. Roy L.A. Crum, "Artificial bubble cloud targets for underwater acoustic remote sensing, J. Atmos. and Ocean Tech. 12, 1289-1302, (1995)

APPENDIX D

HYDROPHONE B&K 8103

Hydrophone Type 8103. A smallsize, high-sensitivity transducer for making absolute sound measurements over the frequency range 0.1Hz to 180 kHz with a receiving sensitivity of .211dB re 1V/⌠Pa. It has a high sensitivity relative to its size and good all-round characteristics which make it generally applicable to laboratory, industrial and investigations of marine animals and in the measurement of the pressure distribution patterns in ultrasonic cleaning educational use. The 8103's high-frequency response is especially valuable when making acoustic baths. It is also useful for cavitation measurements.

Voltage sensitivity*: (with cable) at 20°C	30 µV/Pa ±8 µV (–211 dB re 1 V/µPa ±2 dB)
Charge sensitivity*:	0.12 pC/Pa
Capacitance*: (with integral cable)	3850 pF
Frequency range* (re 250 Hz):	(+1.5 dB) 0.1 Hz to 100 kHz (–6.0 dB) (+3.5 dB) 0.1 Hz to 180 kHz (–12.5 dB)
Dimensions: Length: Body dia:	50 mm (1.97″) 9.5 mm (0.37″)
Weight: (including integral cable)	170 g (0.37 lb)
Integral cable:	6 m waterproof low-noise double-shielded teflon cable with standard miniature coaxial plug

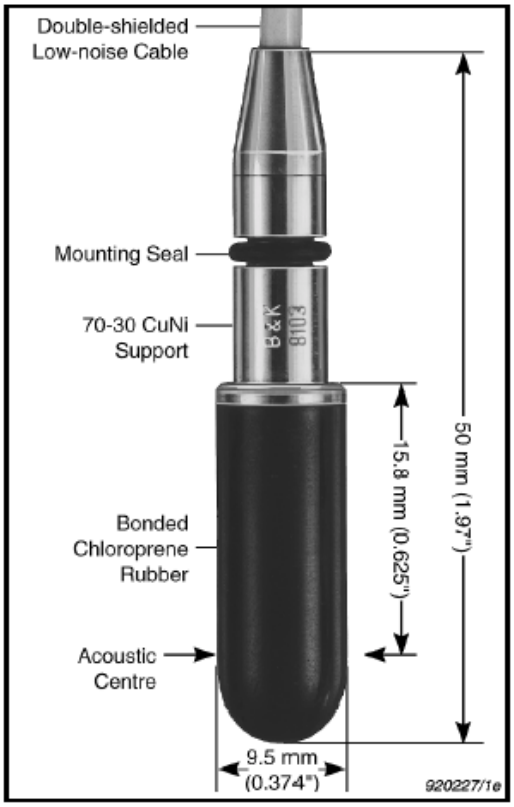

REFERENCES

[1] Kobelev, Yu A., and A.M. Sutin "Difference-frequency sound generation in a liquid containing bubbles of different size", Sov. Phys. Acoust. **26**, 485-487 (1990)

[2] Kozyaev and Naugol'nykh "Parametric sound radiation in a two-phase medium", Sov. Phys. Acoust. **26**, 48-51 (1980)

[3] Wu Junru and Zhu Zhemin "Measurements of effective nonlinearity parameter B/A of water containing trapped cylindrical bubbles", J. Acoust. Soc. Am. **103**, 2960-2961 (1998).

[4] Asada T. "Stable parametric amplification using elastic microcapsules placed in silicone rubber", Jap. J. Appl. Phys., **30**, suppl.30-1, 57-9 (1991).

[5] Herve Pincon "Investigation of a medium with a negative coefficient of nonlinearity", (Master thesis, Georgia Institute of Technology, 2002)

[6] Olivier Pauly "Characterization of a three phase medium with a large and negative parameter of nonlinearity", (Master thesis, Georgia Institute of Technology, 2003).

[7] Robert T. Beyer "Nonlinear acoustic", chap3, 98-100, (1974) Naval Ship System Command, Department of the Navy

[8] Peter J. Westervelt "Parametric acoustic array", J. Acoust. Soc. Am **35**(4),535-537 (1963).

[9] O.V. Rudenko, S.I. Soluyan, and R.V. Khokhlov, "Problems in the theory of nonlinear acoustics", Sov. Phys. Acoustics **20**, 271-275 (1974).

[10] D.H. Trivett and A.L. Van Buren "Propagation of plane, cylindrical and spherical finite amplitude waves", J. Acoust. Soc Am., **69**, 943 (1989)

[11] Akira Nakamura, "Nonlinear behavior of sound and its application to soliton formation", Ultrasonic Symposium,(1988)

[12] Allan D. Pierce "Acoustics, An introduction to its physical principle and applications", Chap 4, 154, (1994), Acoustical Society of America

[13] Young "Roark's formula for stress and strain", Chap10, p440, table24, case 32b, (1989)

[14] Peter Rogers and Van Buren "Standing Wave Parametric Source"